Thanatotranscriptome: genes actively expressed after organismal death

Authors: Alex E. Pozhitkov[1,2], Rafik Neme[2], Tomislav Domazet-Lošo[3,4], Brian G. Leroux[1], Shivani Soni[5], Diethard Tautz[2] and Peter A. Noble[,5,6,7*].

Affiliations:

[1]Department of Oral Health Sciences, University of Washington, Box 357444, Seattle, WA USA 98195.

[2]Max-Planck-Institute for Evolutionary Biology, August-Thienemann-Strasse 2, 24306 Ploen, Germany.

[3]Laboratory of Evolutionary Genetics, Division of Molecular Biology, Ruđer Bošković Institute, 10002 Zagreb, Croatia.

[4]Catholic University of Croatia, Ilica 242, Zagreb, Croatia.

[5]Department of Periodontics, School of Dentistry, University of Washington, Box 357444, Seattle, WA USA 98195.

[6]Department of Biological Sciences, Alabama State University, Montgomery, AL, USA 36101-0271.

[7]PhD Program in Microbiology, Alabama State University, Montgomery, AL, USA 36101-0271.

*Correspondence to:

Peter A. Noble

Email: panoble@washington.edu

Phone: 206-409-6664.

AEP: pozhit@uw.edu

RN: rneme@evolbio.mpg.de

TDL: tdomazet@unicath.hr

BGL: leroux@uw.edu

SS: ssoni@alasu.edu

DT: tautz@evolbio.mpg.edu

Short Title: Transcriptional dynamics after organismal death

1

ABSTRACT

A continuing enigma in the study of biological systems is what happens to highly ordered structures, far from equilibrium, when their regulatory systems suddenly become disabled. In life, genetic and epigenetic networks precisely coordinate the expression of genes -- but in death, it is not known if gene expression diminishes gradually or abruptly stops or if specific genes are involved. We investigated the 'unwinding of the clock' by identifying upregulated genes, assessing their functions, and comparing their transcriptional profiles through postmortem time in two species, mouse and zebrafish. We found transcriptional abundance profiles of 1,063 genes were significantly changed after death of healthy adult animals in a time series spanning from life to 48 or 96 h postmortem. Ordination plots revealed non-random patterns in profiles by time. While most thanatotranscriptome (thanatos-, Greek *defn*. death) transcript levels increased within 0.5 h postmortem, some increased only at 24 and 48 h. Functional characterization of the most abundant transcripts revealed the following categories: stress, immunity, inflammation, apoptosis, transport, development, epigenetic regulation, and cancer. The increase of transcript abundance was presumably due to thermodynamic and kinetic controls encountered such as the activation of epigenetic modification genes responsible for unraveling the nucleosomes, which enabled transcription of previously silenced genes (e.g., development genes). The fact that new molecules were synthesized at 48 to 96 h postmortem suggests sufficient energy and resources to maintain self-organizing processes. A step-wise shutdown occurs in organismal death that is manifested by the apparent upregulation of genes with various abundance maxima and durations. The results are of significance to transplantology and molecular biology.

KEYWORDS

Postmortem transcriptome; postmortem gene expression; Gene meters; calibrated DNA microarrays, thanatotranscriptome; cancer; signaling, development, immunity, apoptosis, transport, inflammation; epigenetic regulation; thermodynamic sink; transplantology, forensic science.

INTRODUCTION

64

65 A healthy adult vertebrate is a complex biological system capable of highly elaborate
66 functions such as the ability to move, communicate, and sense the environment -- all at
67 the same time. These functions are tightly regulated by genetic and epigenetic networks
68 through multiple feedback loops that precisely coordinate the expression of thousands of
69 genes at the right time, in the right place, and in the right level [1]. Together, these
70 networks maintain homeostasis and thus sustain 'life' of a biological system.

71 While much is known about gene expression circuits in life, there is a paucity of
72 information about what happens to these circuits after organismal death. For example, it
73 is not well known whether gene expression diminishes gradually or abruptly stops in
74 death -- nor whether specific genes are newly expressed or upregulated. In organismal
75 'death', defined here as the cessation of the highly elaborate system functions in
76 vertebrates, we conjecture that there is a gradual disengagement and loss of global
77 regulatory networks, but this could result in a regulatory response of genes involved in
78 survival and stress compensation. To test this, we examined postmortem gene expression
79 in two model organisms: the zebrafish, *Danio rerio,* and the house mouse, *Mus musculus.*
80 The purpose of the research was to investigate the "unwinding of the clock" by
81 identifying genes whose expression increases (i.e., nominally upregulated) and assessing
82 their functions based on the primary literature. The biological systems investigated in
83 this study are different from those examined in other studies, such as individual dead
84 and/or injured cells in live organisms, i.e., apoptosis and necrosis (reviewed in refs. [2-
85 5]). In contrast to previous studies, gene expression from the entire *D. rerio* body, and
86 the brains and livers of *M. musculus* were assessed through postmortem time. Gene
87 expression was measured using the 'Gene Meter' approach that precisely reports gene
88 transcript abundances based on a calibration curve for each microarray probe [6].

MATERIALS AND METHODS

90 **Induced death and postmortem incubation.** Zebrafish Forty-four female *Danio rerio*
91 were transferred from several flow-through aquaria kept at $28^{o}C$ to a glass beaker
92 containing 1 L of aquarium water. Four individuals were immediately taken out, snap
93 frozen in liquid nitrogen, and stored in Falcon tubes at $-80^{o}C$ (two zebrafish per tube).
94 These samples were designated as the first set of live controls. A second set of live
95 controls was immersed in an open cylinder (described below). Two sets of live controls
96 were used to determine if putting the zebrafish back into their native environment had
97 any effects on gene expression (we later discovered no significant effects).

98 The rest of the zebrafish were subjected to sudden death by immersion in a "kill"
99 chamber. The chamber consisted of an 8 L styrofoam container filled with chilled ice
100 water. To synchronize the death of the rest of the zebrafish, they were transferred to an
101 open cylinder with a mesh-covered bottom and the cylinder was immersed into the kill
102 chamber. After 20 to 30 s of immersion, four zebrafish were retrieved from the chamber,
103 snap frozen in liquid nitrogen, and stored at $-80^{o}C$ (two zebrafish per Falcon tube). These
104 samples were designated as the second set of live controls. The remaining zebrafish were

3

105 kept in the kill chamber for 5 min and then the cylinder was transferred to a flow-through
106 aquarium kept at 28°C so that they were returned to their native environment.

107 Postmortem sampling of the zebrafish occurred at: time 0, 15 min, 30 min, 1 h, 4 h, 8 h,
108 12 h, 24 h, 48 h, and 96 h. For each sampling time, four expired zebrafish were retrieved
109 from the cylinder, snap frozen in liquid nitrogen, and stored at -80°C in Falcon tubes (two
110 zebrafish to a tube). One zebrafish sample was lost, but extraction volumes were
111 adjusted to one organism.

112 <u>Mouse</u> The mouse strain C57BL/6JRj (Janvier SAS, France) was used for our
113 experiments. The mice were 20-week old males of approximately the same weight. The
114 mice were highly inbred and were expected to have a homogenous genetic background.
115 Prior to euthanasia, the mice were kept at room temperature and were given *ad libitum*
116 access to food and water. Each mouse was euthanized by cervical dislocation and placed
117 in an individual plastic bag with holes to allow air / gas exchange. The bagged carcasses
118 were kept at room temperature in a large, open polystyrene container. Sampling of the
119 deceased mice began at 0 h (postmortem time zero) and continued at 30 min, 1 h, 6 h, 12
120 h, 24 h and 48 h postmortem. At each sample time, 3 mice were sampled (except for 48h
121 where 2 mice were sampled) and the entire brain (plus stem) and two portions of the liver
122 were extracted from each mouse. For liver samples, clippings were taken from the
123 foremost and rightmost lobes of the liver. The brain and liver samples were snap frozen
124 in liquid nitrogen and stored individually in Falcon tubes at -80°C.

125 The euthanasia methods outlined above are approved by the American Veterinary
126 Medical Association (AVMA) Guidelines for Euthanasia (www.avma.org) and carried
127 out by personnel of the Max-Planck-Institute for Evolutionary Biology (Ploen, Germany).
128 All animal work: followed the legal requirements, was registered under number V312-
129 72241.123-34 (97-8/07) and approved by the ethics commission of the Ministerium für
130 Landwirtschaft, Umwelt und ländliche Räume, Kiel (Germany) on 27. 12. 2007.

131 **RNA extraction, labeling, hybridization and DNA microarrays.** The number of
132 biologically distinct organisms was 43 for zebrafish and 20 for mice. Samples from two
133 fish were pooled for analysis, resulting in two replicate measurements at each time point.
134 The number of replicated measurements for mice was three at each of the first six time
135 points and two at 48h. Thus, the total number of samples analyzed was 22 for zebrafish
136 and 20 for mice. For the zebrafish, samples were mixed with 20 ml of Trizol and
137 homogenized using a TissueLyzer (Qiagen). For the mice, 100 mg of brain or liver
138 samples were mixed with 1 ml of Trizol and homogenized. One ml of the emulsion from
139 each sample was put into a fresh 1.5 ml centrifuge tube for RNA extraction and the rest
140 was frozen at -80°C.

141 RNA was extracted by adding 200 µl of chloroform, vortexing the sample, and
142 incubating it at 25°C for 3 min. After centrifugation (15 min at 12000 x g at 4°C), the
143 supernatant (approx. 350 µl) was transferred to a fresh 1.5 ml tube containing an equal
144 volume of 70% ethanol. The tube was vortexed, centrifuged and purified following the
145 procedures outlined in the PureLink RNA Mini Kit (Life Technologies, USA).

146 The isolated RNA, 400 ng per sample, was labeled, purified and hybridized according to
147 the One-Color Microarray-based Gene Expression Analysis (Quick Amp Labeling) with
148 Tecan HS Pro Hybridization kit (Agilent Technologies). For the zebrafish, the labeled

149 RNA was hybridized to the Zebrafish (v2) Gene Expression Microarray (Design ID
150 019161). For the mouse, the labeled RNA was hybridized to the SurePrint G3 Mouse GE
151 8x60K Microarray Design ID 028005 (Agilent Technologies). The microarrays were
152 loaded with 1.65 µg of labeled cRNA for each postmortem sample.

153 **Microarray calibration.** Oligonucleotide (60 nt) probes on the zebrafish and mouse
154 microarrays were calibrated using pooled labeled cRNA of all zebrafish and all mouse
155 postmortem samples, respectively. The dilution series for the Zebrafish array was created
156 using the following concentrations of labeled cRNA: 0.41, 0.83, 1.66, 1.66, 1.66, 3.29,
157 6.60, and 8.26 µg. The dilution series for the Mouse arrays was created using the
158 following concentrations of labeled cRNA: 0.17, 0.33, 0.66, 1.32, 2.64, 5.28, 7.92, and
159 10.40 µg. Calibration involved plotting the signal intensities of the probes against a
160 dilution factor and determining the isotherm model (e.g., Freundlich and/or Langmuir)
161 that best fit the relationship between signal intensities and gene abundances.

162 Consider zebrafish gene transcripts targeted by A_15_P110618 (which happens to be one
163 of the transcriptional profiles of gene *Hsp70.3* shown in Fig 2A). External file
164 FishProbesParameters.txt shows that a Freundlich model best fit the dilution curve with
165 R^2=0.99. The equation for this probe is the following:

166 $$SI = \exp(7.1081)x^{0.67632}$$

167 where *SI* is the observed average signal intensity for dilution *x*. The gene abundance *G*
168 was calculated by inverting this equation. For this probe, signal intensity at each
169 postmortem time, SI_t, is determined by the equation: $G= (SI_t/ \exp(7.1081))^{(1/0.67632)}$.
170 Specifically, consider two biological replicates of 15 min postmortem zebrafish, the
171 signal intensities of the probe A_15_P110618 are 770.5 and 576.0, which translates into
172 the abundances 0.50 and 0.33 arbitrary units (a.u.) respectively. The target abundances
173 were further converted to log10 and are shown in external file Fish_log10_AllProfiles.txt.

174 Details of the calibration protocols to calculate gene expression values, i.e., mRNA
175 relative abundances, are provided in our recent paper where we describe the "Gene
176 Meter" [6].

177 **Statistical analysis**. Abundance levels were log-transformed for analysis to stabilize the
178 variance. A one-sided Dunnett's T-statistic was applied to test for increase at one or more
179 postmortem times compared to live control (fish) or time 0 (mouse). A bootstrap
180 procedure with 10^9 simulations was used to determine the critical value for the Dunnett
181 statistics in order to accommodate departures from parametric assumptions and to
182 account for multiplicity of testing. The profiles for each gene were centered by
183 subtracting the mean values at each postmortem time point to create "null" profiles.
184 Bootstrap samples of the null profiles were generated to determine the 95th percentile of
185 the maximum (over all genes) of the Dunnett statistics. Significant postmortem
186 upregulated genes were selected as those having Dunnett T values larger than the 95th
187 percentile. Only significantly upregulated genes were retained for further analyses.

188 Orthogonal transformation of the abundances to their principal components (PC) was
189 conducted and the results were graphed on a 2 dimensional ordination plot. The *m* x *n*
190 matrix of abundances (sampling times by number of gene transcripts), which is 10 x 548
191 for zebrafish and 7 x 515 for mouse, was used to produce an *m* x *m* matrix D of Euclidean

192   distances between all pairs of sampling times. Principal component analysis (PCA) was
193   performed on the matrix of distances, D. To investigate and visualize differences
194   between the sampling times, a scatterplot of the first two principal components (PC1 and
195   PC2) was created. To establish relative contributions of the gene transcripts, the
196   projection of each sampling time onto the (PC1, PC2) plane was calculated and those
197   genes with high correlations (>=0.70) between abundances and either component (PC1 or
198   PC2) were displayed as a biplot.

199   **Gene annotation and functional categorization.** Microarray probe sequences were
200   individually annotated by performing a BLASTN search of the zebrafish and mouse
201   NCBI databases (February, 2015). The gene annotations were retained if the bit score
202   was greater than or equal to 100 and the annotations were in the correct 5' to 3'
203   orientation. Transcription factors, transcriptional regulators, and cell signaling
204   components (e.g., receptors, enzymes, and messengers) were identified as global
205   regulatory genes. The rest were considered response genes.

206   Functional categorizations were performed by querying the annotated gene transcripts in
207   the primary literature and using UniProt (www.uniprot.org). Genes not functionally
208   categorized to their native organism (zebrafish or mouse) were categorized to genes of
209   phylogenetically related organisms (e.g., human). Cancer-related genes were identified
210   using a previously constructed database (see Additional File 1: Table S1 in [7]).

211

RESULTS

Similar quantities of total mRNA were extracted from zebrafish samples for the first 12 h postmortem (avg. 1551 ng per µl tissue extract) then the quantities abruptly decreased with postmortem time (Table S1). The quantities of total mRNA extracted from the mouse liver samples were about the same for the first 12 h postmortem (avg. of 553 ng per µl tissue extract) then they increased with time (Table S2). The quantities of total mRNA extracted from the mouse brain samples were similar (avg. of 287 ng per µl tissue extract) for all postmortem times (Table S2). Hence, the amount of total mRNA extracted depended of the organism/organ/tissue and time.

Calibration of the microarray probes and determination of the transcript abundances at each postmortem sampling time produced a fine-grain series of data for the zebrafish and the mouse. Approximately 84.3% (36,811 of 43,663) zebrafish probes and 67.1% (37,368 of 55,681) mouse probes were found to provide a suitable dose-response curve for calibration (Files S**Error! Reference source not found.** to S**Error! Reference source not found.**).

Figure 1 shows the sum of all gene abundances calculated from the calibrated probes with postmortem time. In general, the sum of all abundances decreased with time, which means that less targets hybridized to the microarray probes. In the zebrafish, mRNA decreased abruptly at 12 h postmortem (Fig 1A), while for the mouse brain Fig 1B), total mRNA increased in the first hour and then gradually decreased. For the mouse liver, mRNA gradually decreased with postmortem time. The fact that total mRNA shown in Figs 1A and 1B mirrors the electrophoresis banding patterns shown in Fig S1 and S2 (ignoring the 28S and 18S rRNA bands) indicates a general agreement of the Gene Meter approach to another molecular approach (i.e., Agilent Bioanalyzer). Hence, total mRNA abundances depended on the organism (zebrafish, mouse), organ (brain, liver), and postmortem time, which are aligned with previous studies [8,9,10,11,12,13].

Fig 1. Total mRNA abundance (arbitrary units, a.u.) by postmortem time determined using all calibrated microarray probes. A, extracted from whole zebrafish; B, extracted from brain and liver tissues of whole mice. Each datum point represents the mRNA from two organisms in the zebrafish and a single organism in the mouse.

The abundance of a gene transcript is determined by its rate of synthesis and its rate of degradation [14]. We focused on genes that show a significant increase in RNA abundance -- relative to live controls -- because these genes are likely to be actively transcribed in organismal death despite an overall decrease in total mRNA with time. An upregulated transcription profile was defined as one having at least one time point where the abundance was statistically higher than that of the control (Fig 2 A to 2C). It is important to understand that the entire profiles, i.e., 22 data points for the zebrafish and 20 points for the mouse, were subjected to a statistical test to determine significance (see Materials and Methods). We found 548 zebrafish transcriptional profiles and 515 mouse profiles were significantly upregulated. The fact that there are upregulated genes is consistent with the notion that there is still sufficient energy and functional cellular machinery for transcription to occur -- long after organismal death.

255 **Fig 2. Transcriptional profiles of representative genes (a.u.), ordination plots based**
256 **on transcript abundances by postmortem time (h) with corresponding transcript**
257 **contributions (biplots), and averaged transcript abundances by group. (A)**
258 **Transcriptional profile of the *Hsp70.3* gene, (B) the *Tox2* gene, and (C) the NULL**
259 **(i.e., no annotation, probe number shown) gene as a function of postmortem time.**
260 **Each datum point was derived from the mRNA of two zebrafish or one mouse. (D)**
261 **Ordination plots of the zebrafish and (E) mouse were based on all upregulated gene**
262 **profiles by postmortem time (h). Gene transcripts in the biplots were arbitrarily**
263 **assigned alphabetical groups based on their positions in the ordination. The**
264 **average transcript abundances for each group are shown.**

265

266 Based on GenBank gene annotations, we found that among the upregulated genes for the
267 zebrafish, 291 were protein-coding genes (53%) and 257 non-coding mRNA (47%) and,
268 for the mouse, 324 known protein-coding genes (63%), 190 non-coding mRNA (37%),
269 and one control sequence of unknown composition. Hence, about 58% of the total
270 upregulated genes in the zebrafish and mouse are known and the rest (42%) are non-
271 coding RNA.

272 Examples of genes yielding transcripts that significantly increased in abundance with
273 postmortem time are: the 'Heat shock protein' (*Hsp70.3)* gene, the 'Thymocyte selection-
274 associated high mobility group box 2' (*Tox2*) gene, and an unknown (*NULL*) gene (Fig
275 2A to 2C). While the *Hsp70.3* transcript increased after 1 h postmortem to reach a
276 maximum at 12 h, the *Tox2* transcript increased after 12 h postmortem to reach a
277 maximum at 24 h, and the *NULL* transcript consistently increased with postmortem time.
278 These figures provide typical examples of transcript profiles and depict the high
279 reproducibility of the sample replicates as well as the quality of output obtained using the
280 Gene Meter approach.

281 **Non-random patterns in transcript profiles**
282 Ordination plots of the significantly upregulated transcript profiles revealed prominent
283 differences with postmortem time (Fig 2D and 2E), suggesting the expression of genes
284 followed a discernible (non-random) pattern in both organisms. The biplots showed that
285 203 zebrafish transcript profiles and 226 mouse profiles significantly contributed to the
286 ordinations. To identify patterns in the transcript profiles, we assigned them to groups
287 based on their position in the biplots. Six profile groups were assigned for the zebrafish
288 (A to F) and five groups (G to K) were assigned for the mouse. Determination of the
289 average gene transcript abundances by group revealed differences in the shapes of the
290 averaged profiles, particularly the timing and magnitude of peak transcript abundances,
291 which accounted for the positioning of data points in the ordinations.

292 Genes coding for global regulatory functions were examined separately from others (i.e.,
293 response genes). Combined results show that about 33% of the upregulated genes in the
294 ordination plots were involved in global regulation with 14% of these encoding
295 transcription factors/transcriptional regulators and 19% encoding cell signaling proteins
296 such as enzymes, messengers, and receptors (Table S3). The response genes accounted
297 for 67% of the upregulated transcripts.

298 The genes were assigned to 22 categories (File S8) with some genes having multiple
299 categorizations. For example, the Eukaryotic Translation Initiation Factor 3 Subunit J-B
300 (*Eif3j2*) gene was assigned to protein synthesis and cancer categories [15].

301 Genes in the following functional categories were investigated: stress, immunity,
302 inflammation, apoptosis, solute/ion/protein transport, embryonic development, epigenetic
303 regulation and cancer. We focused on these categories because they were common to
304 both organisms and contained multiple genes, and they might provide explanations for
305 postmortem upregulation of genes (e.g., epigenetic gene regulation, embryonic
306 development, cancer). The transcriptional profiles of the genes were plotted by category
307 and each profile was ordered by the timing of the upregulation and peak transcript
308 abundance. This allowed comparisons of gene expression dynamics as a function of
309 postmortem time for both organisms. For each category, we provided the gene name and
310 function and compared expression dynamics within and between the organisms.

311 **Stress response**
312 In organismal death, we anticipated the upregulation of stress response genes because
313 these genes are activated in life to cope with perturbations and to recover homeostasis
314 [16]. The stress response genes were assigned to three groups: heat shock protein (*Hsp*),
315 hypoxia-related, and 'other' responses such as oxidative stress.

316 *Hsp* In the zebrafish, upregulated *Hsp* genes included: 'Translocated promoter region'
317 (*Tpr*), *Hsp70.3,* and *Hsp90* (Fig 3). The *Tpr* gene encodes a protein that facilitates the
318 export of the *Hsp* mRNA across the nuclear membrane [17] and has been implicated in
319 chromatin organization, regulation of transcription, mitosis [18] and controlling cellular
320 senescence [19]. The *Hsp70.3* and *Hsp90* genes encode proteins that control the level of
321 intracellular calcium [20], assist with protein folding, and aid in protein degradation [21].

322 In the mouse, upregulated *Hsp* genes included: *Tpr*, *Hsp*-associated methyltransferase
323 (*Mettl21*) and Heat Shock Protein 1 (*Hspe1*) (Fig 3). The *Mettl21* gene encodes a protein
324 modulating *Hsp* functions [22]. The *Hspe1* gene encodes a chaperonin protein that
325 assists with protein folding in the mitochondria [23].

326 The timing and duration of *Hsp* upregulation varied by organism. In general, activation
327 of *Hsp* genes occurred much later in the zebrafish than the mouse (4 h vs. 0.5 h
328 postmortem, respectively). There were also differences in transcript abundance maxima
329 since, in the zebrafish, maxima were reached at 9 to 24 h, while in the mouse maxima
330 were reached at 12 to 24 h. Previous studies have examined the upregulation of *Hsp70.3*
331 with time in live serum-stimulated human cell lines [24]. In both the zebrafish and
332 human cell lines the *Hsp70.3* gene transcript reached maximum abundance at about 12 h
333 (Fig 2A), indicating the same reactions are occurring in life and death.

334

335 **Fig 3. Upregulated stress response genes by postmortem time (h) and stress**
336 **category. A. zebrafish; B, mouse. Green, intermediate value; Red, maximum value.**

337

Hypoxia

338 *Hypoxia*
339 In the zebrafish, upregulated hypoxia-related genes included: Carbonic anhydrase 4
340 (*Ca4c*), Nuclear factor interleukin-3 (*Nfil3*), Hypoxia-inducible factor 1-alpha (*Hiflab*)
341 and Arginase-2 (*Arg2*) (Fig 3). The Carbonic anhydrase 4 (*Ca4c*) gene encodes an
342 enzyme that converts carbon dioxide into bicarbonate in response to anoxic conditions
343 [25]. The *Nfil3* gene encodes a protein that suppresses hypoxia-induced apoptosis [26]
344 and activates immune responses [27]. The *Hiflab* gene encodes a transcription factor that
345 prepares cells for decreased oxygen [28]. The *Arg2* gene encodes an enzyme that
346 catalyzes the conversion of arginine to urea under hypoxic conditions [29]. Of note, the
347 accumulation of urea presumably triggered the upregulation of the *Slc14a2* gene at 24 h,
348 reported in the Transport Section (below).

349 In the mouse, upregulated hypoxia genes included: Methyltransferase hypoxia inducible
350 domain (*Methig1*) and Sphingolipid delta-desaturase (*Degs2*) (Fig 3). The *Methig1* gene
351 encodes methyltransferase that presumably is involved in gene regulation [30]. The
352 *Degs2* gene encodes a protein that acts as an oxygen sensor and regulates ceramide
353 metabolism [31]. Ceramides are waxy lipid molecules in cellular membranes that
354 regulate cell growth, death, senescence, adhesion, migration, inflammation, angiogenesis
355 and intracellular trafficking [32].

356 The activation of the *Ca4c* gene in the zebrafish indicates a build up of carbon dioxide at
357 0.1 to 1 h postmortem in the zebrafish presumably due lack of blood circulation. The
358 upregulation of the *Nfil3* gene in the zebrafish and *Methig1* gene in the mouse suggests
359 hypoxic conditions existed within 0.5 h postmortem in both organisms. The upregulation
360 of other hypoxia genes varied with postmortem time, with the upregulation of *Hiflab,*
361 *Arg2,* and *Degs2* genes occurring at 4 h, 12 h and 24, respectively.

Other stress responses

362 *Other stress responses*
363 In the zebrafish, upregulated response genes included: Alkaline ceramidase 3 (*Acer3*),
364 Peroxirodoxin 2 (*Prdx2*), Immediate early (*Ier2*), Growth arrest and DNA-damage-
365 inducible protein (*Gadd45a*), Zinc finger CCH domain containing 12 (*Zcchc12*),
366 Corticotropin releasing hormone receptor 1 (*Crhr1*), and Zinc finger AN1-type domain 4
367 (*Zfand4*) (Fig 3). The *Acer3* gene encodes a stress sensor protein that mediates cell-
368 growth arrest and apoptosis [33]. The *Prdx2* gene encodes an antioxidant enzyme that
369 controls peroxide levels in cells [34] and triggers production of *Tnfa* proteins that induce
370 inflammation [35]. The *Ier2* gene encodes a transcription factor involved in stress
371 response [36]. The *Gadd45a* gene encodes a stress protein sensor that stops the cell cycle
372 [37], modulates cell death and survival, and is part of the signaling networks in immune
373 cells [38]. The *Zcchc12* gene encodes a protein involved in stress response in the brain
374 [39]. The *Crhr1* and *Zfand4* genes encode stress proteins [40,41].

375 While the *Acer3, Prdx2,* and *Ier2* genes were activated within 0.3 h postmortem,
376 indicating a changed physiological state; the *Gadd45a* gene was activated at 9 h and the
377 other genes (*Zcchc12, Crhr1, Zfand4*) were activated at 24 h postmortem.

378 In the mouse, upregulated stress response genes included: Membrane-associated RING-
379 CH 4 (*March4*), Homocysteine-responsive endoplasmic reticulum-resident ubiquitin-like
380 domain member 2 (*Herpud2*), Prohibitin-2 (*Phb2*), *Gadd45a*, and Two-oxoglutarate and

381   iron-dependent oxygenase domain-containing 1 (*Ogfod1*) (Fig 3). The *March4* gene
382   encodes an immunologically-active stress response protein [42]. The *Herpud2* gene
383   encodes a protein that senses the accumulation of unfolded proteins in the endoplasmic
384   reticulum [43]. The *Phb2* gene encodes a cell surface receptor that responds to
385   mitochondrial stress [44]. The *Ogfod1* gene encodes a stress-sensing protein [45].

386   Note that the stress genes in the mouse were all activated within 1 h postmortem and
387   remained upregulated for 48 h.

388   *Summary of stress response*
389   In both organisms, organismal death activated heat shock, hypoxia, and other stress
390   genes, which varied in the timing and duration of upregulation within and between
391   organisms. Consider, for example, the *Tpr* and *Gadd45a* genes, which were common to
392   both organisms. While the *Tpr* genes were upregulated within 0.5 h postmortem in both
393   organisms, the *Gadd45a* gene was upregulated at 9 h in the zebrafish and 0.5 h in the
394   mouse. In addition, the transcription profile of the *Tpr* gene was more variable in the
395   zebrafish than the mouse since it was activated at 0.3 h, 9 h and 24 h postmortem, which
396   suggest the gene might be regulated through a feedback loop. In contrast, in the mouse,
397   the *Tpr* gene was upregulated at 0.5 h and the transcripts reached peak abundance at 12
398   and 24 h postmortem.

399   Taken together, the stress genes were activated in both organisms to compensate for a
400   loss in homeostasis.

401   **Innate and adaptive immune responses**
402   In organismal death, we anticipated the upregulation of immune response genes because
403   vertebrates have evolved ways to protect the host against infection in life, even under
404   absolutely sterile conditions [46]. Inflammation genes were excluded from this section
405   (even though they are innate immune genes) because we examined them in a separate
406   section (below).

407   In the zebrafish, upregulated immunity genes included: Early growth response-1 and -2
408   (*Egr1, Egr2*), Interleukin-1b (*Il1b*), L-amino acid oxidase (*Laao*), Interleukin-17c (*Il17c*),
409   Membrane-spanning 4-domains subfamily A member 17A.1 (*Ms4a17.a1*), Mucin-2
410   (*Muc2*), Immunoresponsive gene 1 (*Irg1*), Interleukin- 22 (*Il22*), Ubl carboxyl-terminal
411   hydrolase 18 (*Usp18*), ATF-like 3 (*Batf3*), Cytochrome b-245 light chain (*Cyba*), and
412   'Thymocyte selection-associated high mobility group" box protein family member 2
413   (*Tox2*) (Fig 4). The *Egr1* and *Egr2* genes encode proteins that regulate B and T cell
414   functions in adaptive immunity [47,48]. The *Il1b* gene encodes an interleukin that kills
415   bacterial cells through the recruitment of other antimicrobial molecules [49]. The *Laao*
416   gene encodes an oxidase involved in innate immunity [50]. The *Il17c* and *Il22* genes
417   encode interleukins that work synergically to produce antibacterial peptides [51]. The
418   *Ms4a17.a1* gene encodes a protein involved in adaptive immunity [52]. The *Muc2* gene
419   encodes a protein that protects the intestinal epithelium from pathogenic bacteria [53].
420   The *Irg1* gene encodes an enzyme that produces itaconic acid, which has antimicrobial
421   properties [54]. The *Usp18* gene encodes a protease that plays a role in adaptive
422   immunity [55]. The *Batf3* gene encodes a transcription factor that activates genes
423   involved in adaptive immunity [56]. The *Cyba* gene encodes an oxidase that is used to

424 kill microorganisms [57]. The *Tox2* gene encodes a transcription factor that regulates
425 Natural Killer (NK) cells of the innate immune system [58].

426

427 **Fig 4. Upregulated immunity genes by postmortem time (h). A. zebrafish; B, mouse.**
428 **Green, intermediate value; Red, maximum value. Some transcripts were**
429 **represented by two different probes (e.g. *Il1b, Laao*).**

430

431 Upregulation of immunity genes in the zebrafish occurred at different times with varying
432 durations. While genes involved in adaptive immunity were upregulated at 0.1 to 0.3 h
433 (*Egr*), 9 h (*Ms4a17.a1*) and 24 h (*Usp18, Batf3*) postmortem, genes involved in innate
434 immunity were upregulated at 4 h (*Il1b*), 9 h (*Laao, Il17c*), 12 h (*Muc2, Irg1*) and 24 h
435 (*Il22, Cyba, Tox2*) indicating a multi-pronged and progressive approach to deal with
436 injury and the potential of microbial invasion.

437 In the mouse, upregulated antimicrobial genes included: Catalytic polypeptide-like 3G
438 (*Apobec3g*), CRISPR-associated endonuclease (*Cas1*), Perforin-1 (*Prf1*),
439 Immunoglobulin heavy variable 8-11 (*Ighv8-11*), C4b-binding protein (*C4b*),
440 Complement component C7 (*C7*), T cell receptor alpha and delta chain (*Tcra/Tcrd*), High
441 affinity immunoglobulin gamma Fc receptor I (*Fcgr1a*), Defensin (*Defb30*), Chemokine-
442 4 (*Ccr4*), Interleukin-5 (*Il5*), NK cell receptor 2B4 (*Cd244*), Cluster of differentiation-22
443 (*Cd22*), Lymphocyte cytosolic protein 2 (*Lcp2*), Histocompatibility 2 O region beta locus
444 (*H2ob*) and Interferon-induced transmembrane protein 1 (*Ifitm1*) (Fig 4). The *Apobec3g*
445 gene encodes a protein that plays a role in innate anti-viral immunity [59]. The *Cas1*
446 gene encodes a protein involved in regulating the activation of immune systems
447 [60,61,62,63]. The *Prf1, C7,* and *Defb30* genes encode proteins that kill bacteria by
448 forming pores in the plasma membrane of target cells [64,65,66]. The *Ighv8-11* gene
449 encodes an immunoglobulin of uncertain function. The *C4b* gene encodes a protein
450 involved in the complement system [67]. The *Tcra/Tcrd* genes encode proteins that play
451 a role in the immune response [68]. The *Fcgr1a* gene encodes a protein involved in both
452 innate and adaptive immune responses [69]. The *Ccr4* gene encodes a cytokine that
453 attracts leukocytes to sites of infection [70]. The *Il5* gene encodes an interleukin
454 involved in both innate and adaptive immunity [71,72]. The *Cd244* and *Cd22* genes
455 encode proteins involved in innate immunity [73]. The *Lcp2* gene encodes a signal-
456 transducing adaptor protein involved in T cell development and activation [74]. The
457 *H2ob* gene encodes a protein involved in adaptive immunity. The *Ifitm1* gene encodes a
458 protein that has antiviral properties [75].

459 Most immune response genes were upregulated within 1 h postmortem in the mouse
460 (*n*=14 out of 16 genes), indicating a more rapid response than that of the zebrafish.

461 *Summary of immune response*
462 The upregulated immune response genes in both organisms included innate and adaptive
463 immunity components. An interesting phenomenon observed in the mouse (but not
464 zebrafish) was that four genes (*C7, Tcra/Tcrd, Fcgr1a,* and *Defb30*) reached maximum
465 transcript abundance at two different postmortem times (i.e., 1 h and 12 h) while others

12

466 reached only one maximum. The variability in the gene transcript profiles suggests their
467 regulation is effected by feedback loops.

468 **Inflammation response**

469 We would anticipate the upregulation of inflammation genes in organismal death because
470 inflammation is an innate immunity response to injury. In the zebrafish, upregulated
471 inflammation genes included: *Egr1, Egr2*, *Il1b*, Tumor necrosis factor receptor
472 (*Tnfrsf19*), Heme oxygenase 1 (*Hmox1*), Tumor necrosis factor (*Tnf*), G-protein receptor
473 (*Gpr31*), Interleukin-8 (*Il8*), Tumor necrosis factor alpha (*Tnfa*), Nuclear factor (NF)
474 kappa B (*Nfkbiaa*), MAP kinase-interacting serine/threonine kinase 2b (*Mknk2b*), and
475 Corticotropin-releasing factor receptor 1 (*Crhr1*) (Fig 5). The *Egr1* and *Egr2* genes
476 encode transcription factors that are pro- and anti- inflammatory, respectively [47,48,76].
477 The *Il1b* gene encodes a pro-inflammatory cytokine that plays a key role in sterile
478 inflammation [77,78]. The *Tnfrsf19* gene encodes a receptor that has pro-inflammatory
479 functions [79]. The *Hmox1* gene encodes an enzyme that has anti-inflammatory
480 functions and is involved in Heme catabolism [80,81]. The *Tnf* and *Tnfa* genes encode
481 pro-inflammatory proteins. The *Gpr31* gene encodes a pro-inflammatory protein that
482 activates the NF-kB signaling pathway [82]. The *Il8* gene encodes a cytokine that has
483 pro-inflammatory properties [83]. The *Nfkbiaa* gene encodes a protein that integrates
484 multiple inflammatory signaling pathways including *Tnf* genes [84]. The *Mknk2b* gene
485 encodes a protein kinase that directs cellular responses and is pro-inflammatory [85].
486 The *Crhr1* gene modulates anti-inflammatory responses [86].

487

488 **Fig 5. Upregulated inflammation genes by postmortem time (h). A. zebrafish; B,**
489 **mouse. Inflammation, Pro-, + ; Anti, - . Green, intermediate value; Red, maximum**
490 **value. The *Il1b* and *Mknk2b* genes were represented by two different probes.**

491

492 The upregulation of pro-inflammatory *Egr1* gene at 0.1 h was followed by the
493 upregulation of anti-inflammatory *Egr2* gene at 0.2 h, suggesting the transcription of one
494 gene is affecting the regulation of another (Fig 5). Similarly, the upregulation of the pro-
495 inflammatory *Il1b* gene at 4 h postmortem was followed by: upregulation of pro-
496 inflammatory *Tnfrsf19, Tnf, Gpr31* and *Il8* genes and anti-inflammatory *Hmox1* gene at 9
497 h, the upregulation of pro-inflammatory *Tnfa, Nfkbiaa,* and *Mknk2b* genes at 12 h, and
498 the upregulation of anti-inflammatory *Crhr1* gene at 24 h. Of note, while none of the
499 pro-inflammatory genes were upregulated past 48 h, the anti-inflammatory *Crhr1* gene
500 remained upregulated at 48 h. It should also be noted that the *Il1b, Il8,* and *Tnfa* genes
501 have been reported to be upregulated in traumatic impact injuries in postmortem tissues
502 from human brains [87].

503 In the mouse, upregulated inflammation genes included: mitogen-activated protein kinase
504 (*Map3k2*), TNF receptors (*Tnfrsf9, Tnfrs14*), B-cell lymphoma 6 protein (*Bcl6*), C-C
505 chemokine receptor type 4 (*Ccr4*), Prokineticin-2 (*Prok2*), and platelet-activating factor
506 receptor (*Pafr*) (Fig 5). The *Map3k2* gene encodes a kinase that activates pro-
507 inflammatory NF-kB genes [85]. The *Tnfrsf9* and *Tnfrs14* genes encode receptor
508 proteins that have pro-inflammatory functions [79]. The *Bcl6* gene encodes a

13

509 transcription factor that has anti-inflammatory functions [88]. The *Ccr4* gene encodes a
510 cytokine receptor protein associated with inflammation [70]. The *Prok2 gene* encodes a
511 cytokine-like molecule, while the *Pafr* gene encodes a lipid mediator; both have pro-
512 inflammatory functions [89,90].

513 Most inflammation-associated genes were upregulated within 1 h postmortem and
514 continued to be upregulated for 12 to 48 h. The anti-inflammatory *Bcl6* gene was
515 upregulated at two different times: 0.5 to 6 h and at 24 h suggesting that it is presumably
516 being regulated by a feedback loop. It should also be noted that pro-inflammatory
517 *Map3k2* and *Tnfrs14* genes were not upregulated after 24 and 12 h, respectively, which
518 also suggests regulation by a putative feedback loop from the *Bcl6* gene product.

519 *Summary of inflammation response*
520 In both organisms, some of the upregulated genes have pro-inflammatory functions while
521 others have anti-inflammatory functions, presumably reflecting regulation by feedback
522 loops. The putative feedback loops involve an initial inflammatory reaction followed by
523 an anti-inflammatory reaction to repress it [91]. The variation in the upregulation of
524 these inflammatory genes suggests an underlying regulatory network is involved in
525 organismal death.

526 **Apoptosis and related genes**
527 Since apoptotic processes kill damaged cells for the benefit of the organism as a whole,
528 we anticipated the upregulation of apoptosis genes in organismal death.

529 In the zebrafish, upregulated apoptosis genes included: Jun (*Jdp2, Jun*), Alkaline
530 ceramidase 3 (*Acer3*)*, Fos* (*Fosb, Fosab, Fosl1*), IAP-binding mitochondrial protein A
531 (*Diabloa*), Peroxiredoxin-2 (*Prdx2*), Potassium voltage-gated channel member 1
532 (*Kcnb1*), Caspase apoptosis-related cysteine peptidase 3b (*Casp3b*), DNA-damage-
533 inducible transcript 3 (*Ddit3*), BCL2 (B-cell lymphomas 2)-interacting killer (*Bik*), and
534 Ras association domain family 6 (*Rassf6*) (Fig 6). The *Jdp2* gene encodes a protein that
535 represses the activity of the transcription factor activator protein 1 (*AP-1*) [92]. The
536 *Acer3* gene encodes an enzyme that maintains cell membrane integrity/function and
537 promotes apoptosis [93]. The *Fos* genes encode proteins that dimerize with *Jun* proteins
538 to form part of the *AP-1* that promotes apoptosis [94,95]. The *Diabloa* gene encodes a
539 protein that neutralizes inhibitors of apoptosis (IAP)-binding protein [95] and activates
540 caspases [96]. The *Prdx2* gene encodes antioxidant enzymes that control cytokine-
541 induced peroxide levels and inhibit apoptosis [97]. Although the *Kcnb1* gene encodes a
542 protein used to make ion channels, the accumulation of these proteins in the membrane
543 promotes apoptosis via cell signaling pathway [98]. The *Casp3b* encodes a protein that
544 plays a role in the execution phase of apoptosis [99]. The *Ddit3* gene encodes a
545 transcription factor that promotes apoptosis. The *Bik* gene encodes a protein that
546 promotes apoptosis [100]. The *Rassf6* gene encodes a protein that promotes apoptosis
547 [101].

548

549 **Fig 6. Upregulated apoptosis genes by postmortem time (h). A, zebrafish; B, mouse.**
550 **Apopotosis, Pro, + ; Anti, - . Green, intermediate value; Red, maximum value. The**
551 ***Fosb* gene was represented by two different probes.**

552

553   In the zebrafish, both anti-apoptosis *Jdp2* and pro-apopotosis *Acer3* genes were
554   upregulated within 0.1 h postmortem (Fig 6). The upregulation of these genes was
555   followed by the upregulation of five pro-apoptosis genes and one anti-apoptosis gene
556   within 0.3 to 0.5 h. The transcriptional dynamics varied among the genes. Specifically,
557   (i) the *Fosb* transcript was at low abundance after 1 h, (ii) the *Diabloa* and *Fosab*
558   transcripts reached abundance maxima at 0.5 to 4 h and then were at low abundance after
559   9 h for the *Diabloa* and after 24 h for the *Fosab*, (iii) the *Jun* transcript reached two
560   maxima (one at 0.5 and another at 4 to 12 h) – and after 24 h was at low abundance, (iv)
561   the *Prdx2* transcript showed a continuous increase in abundance, reaching a maximum at
562   24 h and then was at low abundance. The remaining genes were pro-apoptosis and
563   upregulated after 1 to 24 h postmortem. The *Ddit3* and *Rassf6* genes were very different
564   from the other genes in that they were upregulated at one sampling time (12 h and 24 h,
565   respectively) and then the transcripts were at low abundance. Apparently the apoptosis
566   transcripts were at low abundance after 24 h in contrast to the transcripts in other
567   categories (e.g. stress and immunity genes were upregulated for 96 h postmortem).

568   In the mouse, upregulated apoptosis-associated genes included: BCL2-like protein 11
569   (*Bcl2L11*), Casein kinase IIa (*Csnk2a1*), Interleukin 15 receptor subunit a (*Il15ra*),
570   Myocyte enhancer factor 2 (Mef2a), F-box only protein 10 (*Fbxo10*), Sp110 nuclear body
571   protein (*Sp110*), TGFB-induced factor homeobox 1 (*Tgif1*), Intersectin 1 (*Itsm1*) gene,
572   the Ephrin type-B receptor 3 (*Ephb3*), and the p21 protein-activated kinase 4 (*Pak4*) (Fig
573   6). The *Bcl2L11* gene encodes a protein that promotes apoptosis [102]. The *Csnk2a1*
574   gene encodes an enzyme that phosphorylates substrates and promotes apoptosis [103].
575   The *Il15ra* gene encodes an anti-apoptotic protein [104]. The *Mef2a* gene encodes a
576   transcription factor that prevents apoptosis [105]. The *Fbxo10* gene encodes a protein
577   that promotes apoptosis [106]. The *Sp110* gene encodes a regulator protein that promotes
578   apoptosis [107]. The *Tgif1* gene encodes a transcription factor that blocks signals of the
579   transforming growth factor beta (*TGFβ*) pathway; and therefore, is pro-apoptosis [108].
580   The *Itsn1* gene encodes an adaptor protein that is anti-apoptosis [109]. The *Ephb3* gene
581   encodes a protein that binds ligands on adjacent cells for cell signaling and suppresses
582   apoptosis [104]. The *Pak4* gene encodes a protein that delays the onset of apoptosis
583   [110].

584   In the mouse, pro- and anti-apoptosis genes were upregulated within 0.5 h postmortem –
585   however, with exception to *Bcl2L11*, most reached transcript abundance maxima at 12 to
586   48 h postmortem (Fig 6). The *Bcl2L11* transcripts reached abundance maxima at 1 and 6
587   h postmortem.

588   ***Summary of apoptotic response***
589   In both organisms, pro- and anti-apoptosis genes were upregulated in organismal death.
590   However, the timings of the upregulation, the transcript abundance maximum, and the
591   duration of the upregulation varied by organism. The results suggest the apoptotic genes
592   and their regulation are distinctly different in the zebrafish and the mouse, with the
593   mouse genes being upregulated up to 48 h postmortem, while zebrafish genes are
594   upregulated for 24 h. Nonetheless, the pro- and anti-apoptosis genes appear to be inter-
595   regulating each another.

15

Transport gene response

Transport processes maintain ion/solute/protein homeostasis and are involved in influx/efflux of carbohydrates, proteins, signaling molecules, and nucleic acids across membranes. We anticipated that transport genes should be upregulated in organismal death in response to dysbiosis.

In the zebrafish, upregulated transport-associated genes included: Solute carrier family 26 Anion Exchanger Member 4 (*Slc26a4*), Potassium channel voltage gated subfamily H (*Kcnh2*), Transmembrane Emp24 domain containing protein 10 (*Tmed10*), Leucine rich repeat containing 59 (*Lrrc59*), the Nucleoprotein TPR (*Tpr*), Importin subunit beta-1 (*Kpnb1*), Transportin 1 (*Tnpo1*), Syntaxin 10 (*Stx10*) and Urea transporter 2 (*Slc14a2*) (Fig 7). Of note, the four *Tmed10* transcripts shown in Fig 7, each represents a profile targeted by an independent probe. The transcription profiles of this gene were identical, indicating the high reproducibility of the Gene Meter approach. The *Slc26a4* gene encodes prendrin that transports negatively-charged ions (i.e., Cl⁻, bicarbonate) across cellular membranes [111]. The *Kcnh2* gene encodes a protein used to make potassium channels and is involved in signaling [112]. The *Tmed10* gene encodes a membrane protein involved in vesicular protein trafficking [113]. The *Lrrc59, Tpr, Tnpo1,* and *Kpnb1* genes encode proteins involved in trafficking across nuclear pores [114,115,116,117]. The *Stx10* gene encodes a protein that facilitates vesicle fusion and intracellular trafficking of proteins to other cellular components [118]. The *Slc14a2* gene encodes a protein that transports urea out of the cell [119].

Fig 7. Upregulated transport genes by postmortem time (h) and stress category. A. zebrafish; B, mouse. Green, intermediate value; Red, maximum value. The *Tmed10* gene was represented by four different probes.

The *Slc26a4, Kcnh2, Lrrc59* and *Tpr* genes were initially upregulated within 0.3 h postmortem and continue to be expressed for 12 to 24 h. The *Tnpo1* gene was upregulated at two times: 4 h and 12 h suggesting putative regulation by a feedback loop. The remaining genes were upregulated at 24 h. The upregulation of the *Slc14a2* gene suggests a build up of urea in zebrafish cells at 24 to 96 h postmortem, which could be due to the accumulation of urea under hypoxic conditions by the *Arg2* gene (see *Hsp* stress response section).

In the mouse, the following transport-associated genes were upregulated: Calcium-bind mitochondrial carrier protein (*Aralar2*), Sodium-coupled neutral amino acid transporter 4 (*Slc38a4*), SFT2 domain containing 1 (*Sft2d1*), Uap56-interacting factor (*Fyttd1*), Solute carrier family 5 (sodium/glucose co-transporter) member 10 (*Slc5a10*), Mitochondrial import receptor subunit (*Tom5*), 'Translocated promoter region' (*Tpr*), ATP-binding cassette transporter 12 (*Abca12*), Multidrug resistant protein 5 (*Abc5*), LIM and SH3 domain-containing protein (*Lasp1*), Chromosome 16 open reading frame 62 (*C16orf62*), Golgi transport 1 homolog A (*Golt1a*), ATP-binding cassette transporter transporter 17 (*Abca17*), Nucleotide exchange factor (*Sil1*), Translocase of inner mitochondrial membrane 8A1 (*Timm8a1*), Early endosome antigen 1 (*Eea1*), and Potassium voltage-gated channel subfamily V member2 (*Kcnv2*) (Fig 7). The *Aralar2* gene encodes a

640   protein that catalyzes calcium-dependent exchange of cytoplasmic glutamate with
641   mitochondrial aspartate across the mitochondrial membrane and may function in the urea
642   cycle [120]. The *Slc38a4* gene encodes a symport that mediates transport of neutral
643   amino acids and sodium ions [121]. The *Sft2d1* gene encodes a protein involved in
644   transporting vesicles from the endocytic compartment of the Golgi complex [122]. The
645   *Fyttd1* gene is responsible for mRNA export from the nucleus to the cytoplasm [123].
646   The *Slc5a10* gene encodes a protein that catalyzes carbohydrate transport across cellular
647   membranes [124]. The *Tom5* gene encodes a protein that plays a role in importation to
648   proteins destined to mitochondrial sub-compartments [125]. The *Abca12*, *Abca17* and
649   *Abc5* genes encode proteins that transport molecules across membranes [126,127,128].
650   The *Lasp1* gene encodes a protein that regulates ion-transport [129]. The *C16orf62* gene
651   encodes a protein involved in protein transport from the Golgi apparatus to the cytoplasm
652   [130]. The *Golt1a* gene encodes a vesicle transport protein [122]. The *Sil1* gene encodes
653   a protein involved in protein translocation into the endoplasmic reticulum [131]. The
654   *Timm8a1* gene encodes a protein that assists importation of other proteins across inner
655   mitochondrial membranes [132]. The *Eea1* gene encodes a protein that acts as a
656   tethering molecule for vesicular transport from the plasma membrane to the early
657   endosomes [133]. The *Kcnv2* gene encodes a membrane protein involved in generating
658   action potentials [134].

659   Within 0.5 h postmortem, genes involved in: (i) ion and urea regulation (*Aralar*), (ii)
660   amino acid (*Slc38a4*), carbohydrate (*Slc5a10*), and protein (*Sft2d1, Tom5*) transport, (iii)
661   mRNA nuclear export (*Fyttd1, Tpr*), and (iv) molecular efflux (*Abca12, Abc5*) were
662   upregulated in the mouse. The transcription profiles of these genes varied in terms of
663   transcript abundance maxima and duration of the upregulation. While the transcripts of
664   *Aralar, Sft2d1, Slc38a4, Fyttd1* and *Slc5a10* reached abundance maxima at 1 h, those of
665   *Tom5, Tpr, Abca12,* and *Abc5* reached maxima at 12 to 24 h postmortem. The duration
666   of the upregulation also varied for these genes since most were upregulated for 48 h
667   postmortem, while the *Sft2d1, Fyttd1* and *Slc5a10* were upregulated from 0.5 to 12 h or
668   more. The shorter duration of upregulation suggests prompt gene repression. The
669   transcript abundance of *Lasp1, C16orf62, Golt1a,* and *Abca17* increased at 1 h
670   postmortem and remained elevated for 48 h. The transcripts of *Sil1, Timm8a1, Eea1*
671   increased in abundance at 6 h, while those of *Kcnv2* increased at 24 h postmortem and
672   remained elevated for 48 h.

673   ***Summary of transport genes***
674   The upregulation of transport genes suggests attempts by zebrafish and mice to
675   reestablish homeostasis. Although half of these genes were upregulated within 0.5 h
676   postmortem, many were upregulated at different times and for varying durations. While
677   most of the transport gene transcripts in the zebrafish were at low abundance after 24 h,
678   most transport gene transcripts in the mouse remained at high abundance at 24 to 48 h
679   postmortem.

680   **Development genes**
681   An unexpected finding in this study was the discovery of upregulated development genes
682   in organismal death. Most development genes are involved at the early stage of

683 development in the zebrafish and mouse; therefore, we did not anticipate their
684 upregulation in organismal death.

685 In the zebrafish, upregulated development genes included: LIM domain containing
686 protein 2 (*Limd2*), Disheveled-associated activator of morphogenesis 1 (*Daam1b*),
687 Meltrin alpha (*Adam12*), Hatching enzyme 1a (*He1a*), Midnolin (*Midn*), Immediate early
688 response 2 (*Ier2*), Claudin b (*Cldnb*), Regulator of G-protein signaling 4-like (*Rgs4*),
689 Proline-rich transmembrane protein 4 (*Prrt4*), Inhibin (*Inhbaa*), Wnt inhibitory factor 1
690 precursor (*Wif1*), Opioid growth factor receptor (*Ogfr*), Strawberry notch homolog 2
691 (*Sbno2*), and Developing brain homeobox 2 (*Dbx2*) (Fig 8). The *Limd2* gene encodes a
692 binding protein that plays a role in zebrafish embryogenesis [135]. The *Daam1b* gene
693 regulates endocytosis during notochord development [136]. The *Adam12* gene encodes a
694 metalloprotease-disintegrin involved in myogenesis [137]. The *He1a* gene encodes a
695 protein involved in egg envelope digestion [138]. The *Midn* gene encodes a nucleolar
696 protein expressed in the brain and is involved in the regulation of neurogenesis [139,140].
697 The *Ier2* gene encodes a protein involved in left-right asymmetry patterning in the
698 zebrafish embryos [141]. The *Cldnb* gene encodes a tight junction protein in larval
699 zebrafish [142]. The *Rgs4* gene encodes a protein involved in brain development [143].
700 The *Prrt4* gene encodes a protein that is predominantly expressed in the brain and spinal
701 cord in embryonic and postnatal stages of development. The *Inhbaa* gene encodes a
702 protein that plays a role in oocyte maturation [144]. The *Wif1* gene encodes a WNT
703 inhibitory factor that controls embryonic development [145]. The *Ogfr* gene plays a role
704 in embryonic development [146]. The *Sbno2* gene plays a role in zebrafish
705 embryogenesis [147]. The *Dbx2* gene encodes a transcription factor that plays a role in
706 spinal cord development [148].

707

708 **Fig 8. Upregulated development genes by postmortem time (h) and stress category.**
709 **A. zebrafish; B, mouse. Green, intermediate value; Red, maximum value. The**
710 ***Cldnb* gene was represented by two different probes.**

711

712 Although the abundances of *Limd2, Daam1, Adam12, and He1a* transcripts increased in
713 the zebrafish within 0.1 h postmortem, other gene transcripts in this category increased
714 from 0.3 to 24 h postmortem reaching abundance maxima at 24 h or more.

715 In the mouse, development genes were upregulated included: MDS1 and EVI1 complex
716 locus protein EVI1 (*Mecom*), MAM domain containing glycosylphosphatidylinositol
717 anchor 2 (*Mdga2*), FYVE, RhoGEF and PH domain containing 5 (*Fgd5*), RNA binding
718 motif protein 19 (*Rbm19*), Chicken ovalbumin upstream promoter (*Coup*), Single minded
719 homolog 2 (*Sim2*), Solute carrier family 38, member 4 (*Slc38a4*), B-cell lymphoma 6
720 protein (*Bcl6*), Sema domain transmembrane domain (TM) cytoplasmic domain
721 (semaphorin) 6D (*Sema6d*), RNA binding motif protein 45(*Rbm45*), Transcription factor
722 E2F4 (*E2f4*), Long chain fatty acid- CoA Ligase 4 (*Lacs4*), Kallikrein 1-related peptidase
723 b3 (*Klk1b3*), Sema domain, Immunoglobulin domain, transmembrane domain and short
724 cytoplasmic domain (*Sema4c*), TGFB-induced factor homeobox 1 (*Tgif1*), Interferon
725 regulatory factor 2-binding protein-like (*Irf2bpl*), Ephrin type-B receptor 3 (*Ephb3*),
726 Testis-specific Y-encoded-like protein 3 (*Tspyl3*), Protein ripply 3(*Ripply3*), Src kinase-

18

727 associated phosphoprotein 2 (Skap2), DNA polymerase zeta catalytic subunit (*Rev3l*),
728 MKL/Myocardin-Like 2 (*Mkl2*), and Protein phosphatase 2 regulatory subunit A
729 (*Ppp2r1a*) (Fig 8). The *Mecom* gene plays a role in embryogenesis and development
730 [149]. The *Mdga2* gene encodes immunoglobins involved in neural development [150].
731 The *Fgd5* gene is needed for embryonic development since it interacts with
732 hematopoietic stem cells [151]. The *Rbm19* gene is essential for preimplantation
733 development [152]. The *Coup* gene encodes a transcription factor that regulates
734 development of the eye [153] and other tissues [154]. The *Sim2* gene encodes a
735 transcription factor that regulates cell fate during midline development [155]. The
736 *Slc38a4* gene encodes a regulator of protein synthesis during liver development and plays
737 a crucial role in fetal growth and development [156,157]. The *Bcl6* gene encodes a
738 transcription factor that controls neurogenesis [158]. The *Sema6d* gene encodes a protein
739 involved in retinal development [159]. The *Rbm45* gene encodes a protein that has
740 preferential binding to poly(C) RNA and is expressed during brain development [160].
741 The *E2f4* gene is involved in maturation of cells in tissues [161]. The *Lacs4* gene plays a
742 role in patterning in embryos [162]. The *Klk1b3* gene encodes a protein that plays a role
743 in developing embryos [163]. The *Sema4c* gene encodes a protein that has diverse
744 functions in neuronal development and heart morphogenesis [164, 165]. The *Tgif1* gene
745 encodes a transcription factor that plays a role in trophoblast differentiation [166]. The
746 *Irf2bpl* gene encodes a transcriptional regulator that plays a role in female
747 neuroendocrine reproduction [167]. The *Ephb3* gene encodes a kinase that plays a role in
748 neural development [168]. The *Tspyl3* gene plays a role in testis development [169].
749 The *Ripply3* gene encodes a transcription factor involved in development of the ectoderm
750 [170]. The *Skap2* gene encodes a protein involved in actin reorganization in lens
751 development [171]. The *Rev3l* gene encodes a polymerase that can replicate past certain
752 types of DNA lesions and is necessary for embryonic development [172]. The *Mkl2* gene
753 encodes a transcriptional co-activator is involved in the formation of muscular tissue
754 during embryonic development [173]. The *Ppp2r1a* gene plays a role in embryonic
755 epidermal development [174].

756 While the *Mecom, Mdga2, Fgd5, Rbm19, Coup, Sim2, Slc38a4, Bcl6, Sema6d, Rbm45,*
757 *E2f4* and *Lacs4* genes were upregulated within 0.5 h postmortem, the other genes were
758 upregulated at 1 h to 48 h with most transcripts reaching abundance maxima at 12 h or
759 more.

760 *Summary of development genes*
761 In organismal death, there is progressive activation of developmental genes suggesting
762 that they are no longer silenced. A possible reason for this activation is that postmortem
763 physiological conditions resemble those during development.

764 **Cancer genes**
765 There are a number of databases devoted to cancer and cancer-related. Upon cross-
766 referencing the genes found in this study, we discovered a significant overlap. The genes
767 found in this search are presented below.

768 In the zebrafish, the following cancer genes were upregulated: *Jdp2*, xanthine
769 dehydrogenase (*Xdh*), *Egr1, Adam12*, myosin-IIIa (*Myo3a*), *Fosb, Jun*, Integrin alpha 6b
770 (*Itga6*), *Ier2, Tpr*, Dual specificity protein phosphatase 2 (*Dusp2*), Disintegrin and

19

771 metallopeptidase domain 28 (*Adam28*), *Tnpo1,* Ral guanine nucleotide dissociation
772 stimulator-like (*Rgl1*), Carcinoembryonic antigen-related cell adhesion molecule 5
773 (*Ceacam1*), *Fosl1, Il1b, Hif1a,* Serine/threonine-protein phosphatase 2A regulatory
774 (*Ppp2r5d*), DNA replication licensing factor (*Mcm5*), *Gadd45,* Myosin-9 (*Myh9*), *Casp3,*
775 *Tnf, Il8,* Cyclic AMP-dependent transcription factor (*Atf3*), small GTPase (*RhoA*),
776 *Mknk2,* Ephrin type-A receptor 7 precursor (*Epha7*), ETS-related transcription factor
777 (*Elf3*), *Nfkbia, Kpnb1, Wif1,* RAS guanyl-releasing protein 1 (*Rasgrp*), Ras association
778 domain-containing protein 6 (*Rassf6*), *Cyba,* DNA-damage-inducible transcript 3 (*Ddit3*),
779 Serine/threonine-protein kinase (*Sbk1*), and Tyrosine-protein kinase transmembrane
780 receptor (*Ror1*) (Fig 9).

781

782 **Fig 9. Upregulated cancer genes by postmortem time (h). A, Zebrafish; B, Mouse.**
783 **Green, intermediate value; Red, maximum value. Bold gene name means it was**
784 **found in more than one cancer database. The *Rgl1* gene was represented by two**
785 **different probes.**

786

787 In the mouse, the following cancer genes were upregulated: retinoblastoma-like protein 1
788 (*Rbl1*), Elongation factor RNA polymerase II (*Ell*), Bcl-2-like protein 11 (*Bcl2l11*), Sal-
789 like protein 1 (*Sall1*), *Map3k2, Bcl6, Tnfrsf9,* CK2 target protein 2 (*Csnk2a1*),
790 Transcription factor E2f4 (*E2f4*), Zinc finger DHHC-type containing 14 (*Zdhhc14*), *Tpr,*
791 RAS p21 protein activator 1 (*Rasa1*), *Gadd45,* prohibitin (*Phb2*), Serine/threonine-
792 protein phosphatase PP1-gamma catalytic (*Ppp1cc*), *Lasp1,* G protein-coupled receptor
793 kinase 4 (*Grk4*), LIM domain transcription factor (*Lmo4*), Protein phosphatase 1E
794 (*Ppm1e*), Protein sprouty homolog 1 (*Spry1*), Multiple PDZ domain protein (*Mpdz*),
795 Kisspeptin receptor (*Kiss1*), Receptor-type tyrosine-protein phosphatase delta precursor
796 (*Ptprd*), Small effector protein 2-like (*Cdc42*), AT-rich interactive domain-containing
797 protein 1A (*Arid1a*), Lymphocyte cytosolic protein 2 (*Lcp2*), DNA polymerase zeta
798 catalytic subunit (*Rev3l*), *Tnfrsf14,* Integrin beta-6 precursor (*Itgb6*), Triple functional
799 domain protein (*Trio*), ATPase class VI type 11C (*Atp11c*), and Serine/threonine-protein
800 phosphatase 2A regulatory (*Ppp2r1a*) (Fig 9).

801 *Summary of cancer genes*
802 These genes were classified as "cancer genes" in a Cancer Gene Database [7] (Fig 9).
803 The timing, duration and peak transcript abundances differed within and between
804 organisms. Note that some transcripts had two abundance maxima. In the zebrafish, this
805 phenomenon occurred for *Adam12, Jun, Tpr, Dusp2, Tnpo1,* and *Hif1a* and in the mouse,
806 *Bcl6, Tnfrs9, Lasp1, Cdc42,* and *Lcp2*, and is consistent with the notion that the genes are
807 being regulated through feedback loops.

808 **Epigenetic regulatory genes**
809 Epigenetic regulation of gene expression involves DNA methylation and histone
810 modifications of chromatin into active and silenced states [175]. These modifications
811 alter the condensation of the chromatin and affect the accessibility of the DNA to the
812 transcriptional machinery. Although epigenetic regulation plays important role in
813 development, modifications can arise stochastically with age or in response to

814   environmental stimuli [176]. Hence, we anticipated that epigenetic regulatory genes
815   should be involved in organismal death.

816   In the zebrafish, the following epigenetic genes were upregulated: Jun dimerization
817   protein 2 (*Jdp2*), Chromatin helicase protein 3 (*Chd3*), Glutamate-rich WD repeat-
818   containing protein 1 (*Grwd1*), Histone H1 (*Histh1l*), Histone cluster 1, H4-like
819   (*Hist1h46l3*) and Chromobox homolog 7a (*Cbx7a*) (Fig 10). The *Jdp2* gene is thought to
820   inhibit the acetylation of histones and repress expression of the c-Jun gene [177]. The
821   *Chd3* gene encodes a component of a histone deacetylase complex that participates in the
822   remodeling of chromatin [178]. The *Grwd1* gene is thought to be a histone-binding
823   protein that regulates chromatin dynamics at the replication origin [179]. The *Histh1l*
824   gene encodes a histone protein that binds the nucleosome at the entry and exit sites of the
825   DNA and the *Hist1h46l3* gene encodes a histone protein that is part of the nucleosome
826   core [180]. The *Cbx7a* gene encodes an epigenetic regulator protein that binds non-
827   coding RNA and histones and represses gene expression of a tumor suppressor [181].

828

829   **Fig 10. Upregulated epigenetic genes by postmortem time (h). A, Zebrafish; B,**
830   **Mouse. Green, intermediate value; Red, maximum value. Bold gene name means it**
831   **was found in more than one cancer database. The *Jdp2* gene was represented by two**
832   **different probes.**

833

834   Both *Jdp2* and *Chd3* genes were upregulated within 0.3 h postmortem, with their
835   transcripts reaching abundance maxima at 0.5 h. Note that two different probes targeted
836   the *Jdp2* transcript. The *Grwd1* gene was upregulated at 1 h and 24 h postmortem. The
837   histone genes were upregulated at 4 h postmortem with their transcripts reaching
838   abundance maxima at 24 h. The *Cbx7a* gene was upregulated at 12 h and its transcript
839   reached an abundance maximum at 24 h. Transcripts of these genes were at low
840   abundance after 24 h.

841   In the mouse, the following epigenetic genes were upregulated: Tubulin tyrosine ligase-
842   like family member 10 (*Ttll10*), Histone cluster 1 H3f (*Hist1h3f*), Histone cluster 1 H4c
843   (*Hist1h4c*), YEATS domain containing 2 (*Yeats2*), Histone acetyltransferase (*Kat7*), and
844   Probable JmjC domain-containing histone demethylation protein 2C (*Jmjd1c*) (Fig 10).
845   The *Ttll10* gene encodes a polyglycylase involved in modifying nucleosome assembly
846   protein 1 that affects transcriptional activity, histone replacement, and chromatin
847   remodeling [182]. The *Hist1h3f* and *Hist1h4c* genes encode histone proteins are the core
848   of the nucleosomes [183]. The *Yeats2* gene encodes a protein that recognizes histone
849   acetylations so that it can regulate gene expression in the chromatin [184]. The *Kat7*
850   gene encodes an acetyltransferase that is a component of histone binding origin-of-
851   replication complex, which acetylates chromatin and therefore regulates DNA replication
852   and gene expression [185]. The *Jmjd1c* gene encodes an enzyme that specifically
853   demethylates 'Lys-9' of histone H3 and is implicated in the reactivation of silenced genes
854   [186].

855   The *Ttll10, Yeats2* and histone protein genes were upregulated 0.5 h postmortem but their
856   transcripts reached abundance maxima at different times with the *Ttll10* transcript

857 reaching a maximum at 1 to 6 h, the histone transcripts reaching maxima at 6 and 12 h
858 postmortem, and the *Yeats2* transcript reaching maxima at 12 to 24 h postmortem (Fig
859 10). The *Kat7* and *Jmjd1c* genes were upregulated at 24 h and their transcripts reached
860 abundance maxima at 48 h postmortem.

861 *Summary of epigenetic regulatory genes*
862 The upregulation of genes encoding histone proteins, histone-chromatin modifying
863 proteins, and proteins involved in regulating DNA replication at the origin were common
864 to the zebrafish and the mouse. These findings indicate that epigenetic regulatory genes
865 are modifying chromatin structure by regulating the accessibility of transcription factors
866 to the promoter or enhancer regions in organismal death.

867 **Percentage of upregulated genes with postmortem time**

868 The % of upregulated genes was defined as the number of upregulated genes at a specific
869 postmortem time over the total number of upregulated genes in a category. A
870 comparison of the % of upregulated genes by postmortem time of all upregulated genes
871 revealed similarities between the zebrafish and the mouse. Specifically, most genes were
872 upregulated between 0.5 to 24 h postmortem, and after 24 h, the upregulation of most
873 genes stopped (Fig 11, "All genes"). It should be noted that the same pattern was found
874 in stress, transport and development categories for both organisms. However, in the
875 zebrafish, the immunity, inflammation, apoptosis and cancer categories differed from the
876 mouse. Specifically, the genes in the immunity, inflammation, and cancer categories
877 were upregulated much later (1 to 4 h) in the zebrafish than the mouse, and the duration
878 of upregulation was much shorter. For example, while 90% of the genes in the immunity
879 and inflammation categories were upregulated in the mouse within 1 h postmortem, less
880 than 30% of the genes were upregulated in the zebrafish (Fig 11), indicating a slower
881 initial response. It should be noted that while the number of upregulated immunity genes
882 reaching transcript abundance maxima occurred at 24 h postmortem in both organisms,
883 the number of inflammation genes reaching transcript abundance maxima occurred at 1 to
884 4 h in the mouse, and 24 h in the zebrafish. The significance of these results is that the
885 inflammation response occurs rapidly and robustly in the mouse while in the zebrafish, it
886 takes longer to establish, which could be attributed to phylogenetic differences. There
887 were significant differences in the upregulation of apoptosis genes between the zebrafish
888 and the mouse. In the mouse, the number of upregulated apoptosis genes reached 100%
889 at 1 h postmortem and remained sustained for 48 h postmortem while the % of
890 upregulated genes in the zebrafish never reached 70% and gene upregulation was
891 abruptly stopped after 12 h.

892

893 **Fig 11. % of upregulated genes by postmortem time and category. Number of total**
894 **genes by organism and category are shown. "All genes" refers to the genes that**
895 **significantly contributed to the ordination plots. Mouse is red; Zebrafish is black.**

896

DISCUSSION

Active gene expression or residual transcription levels?

One could argue that our study identifies only residual transcription levels of pre-synthesized mRNA (rather than newly-synthesized mRNA) in dead tissues that happen to be enriched with postmortem time. In other words, the observed upregulation of genes may be viewed as an artifact merely reflecting the "enrichment of specific mRNA transcripts" (e.g. stable mRNA) with time. The data, however, does not support this idea because if it were true, one would expect stable transcripts to monotonically increase with time, as they become more enriched (higher abundances) with postmortem time. The data show that the transcripts of most upregulated genes did not display monotonic behavior; rather, the transcripts reached abundance maximum (peak) or maxima (peaks) at various postmortem times (Fig 2D and 2E). This finding should not be a surprise because a statistical procedure was implemented to detect genes that were significantly upregulated – which is essentially selecting gene transcriptional profiles that had peaks. The statistics for the procedure was calibrated with more than a billion simulations. The simulation process corrected for multiple comparisons. The residual transcription level and enrichment idea is also not supported by transcriptional profiles displaying an up-, down-, and up- regulation pattern, which putatively indicates feedback loops (Fig S3). Similarly, simple differential decay rates of mRNAs would not display this pattern because a transcript cannot be stable at one postmortem time, unstable at a subsequent time, and then stable again. A mRNA transcript is either stable or it is not. In conclusion, the gene profiles showing upregulation are the results of active transcription.

It should be noted that postmortem upregulation of genes has been previously reported in cadavers. Using reverse transcription real-time quantitative PCR (RT-RTqPCR), a study showed significant increases in expression of myosin light chain 3 (*Myl3*), matrix metalloprotease 9 (*Mmp9*), and vascular endothelial growth factor A (*Vegfa*) genes in body fluids after 12 h postmortem (187). Interestingly, postmortem upregulation of myosin-related and matrix metalloprotease genes was also found in our study. Specifically, the myosin-related genes included: Myosin-Ig (*Myo1g)* in the mouse*,* and Myosin-IIIa (*Myo3a*) and Myosin-9 (*Myh9*) in the zebrafish. The matrix metalloproteinase gene included the metalloproteinase-14 (*Mmp14b*) gene in the zebrafish. The *Myo1g* gene encodes a protein regulating immune response (189), the Myosin-IIIa (*Myo3a*) gene encodes an uncharacterized protein, the Myosin-9 (*Myh9*) gene encodes a protein involved in embryonic development (190), and the *Mmp14b* gene encodes an enzyme regulating cell migration during zebrafish gastrulation (188). The *Myo1g, Myh9* and *Mmp14b* transcripts increased right after death and reached abundance maxima at 24 h postmortem, while the *Myo3a* transcript reached an abundance maximum at 12 h postmortem. The significance of these results is two-fold: (i) two different technologies (RT-RTqPCR and Gene Meters) have now demonstrated active postmortem upregulation of genes and this expression has now been reported in three organisms (human, zebrafish, and mouse), and (ii) there might be significant overlap in genes upregulated in death as we have showed with myosin- and matrix metalloprotease genes, which warrants further studies using other vertebrates. The purpose of such studies

941 would be to understand common mechanisms involved in the shutdown of highly ordered
942 biological systems.

Why study gene expression in death?

944 The primary motivation for the study was driven by curiosity in the processes of shutting
945 down a complex biological system – which has received little attention so far. While the
946 development of a complex biological system requires time and energy, its shutdown and
947 subsequent disassembly entails the dissipation of energy and unraveling of the complex
948 structures, which does not occur instantaneously and could provide insights into
949 interesting paths. Moreover, other fields of research have examined the shutdown of
950 complex systems (e.g., societies [191], government [192], electrical black outs [193]).
951 Yet, to our knowledge, no study has examined long-term postmortem gene expression of
952 vertebrates kept in their native conditions. The secondary motivation for the study was to
953 demonstrate the precision of Gene Meter technology for gene expression studies to
954 biologists who believe that high throughput DNA sequencing is the optimal approach.

Thermodynamic sinks

956 We initially thought that sudden death of a vertebrate would be analogous to a car driving
957 down a highway and running out of gas. For a short time, engine pistons will move up
958 and down and spark plugs will spark -- but eventually the car will grind to a halt and
959 "die". Yet, in our study we find hundreds of genes are upregulated many hours
960 postmortem, with some (e.g., *Kcnv2, Pafr, Degs2, Ogfod1, Ppp2rla, Ror1,* and *Iftm1*)
961 upregulated days after organismal death. This finding is surprising because in our car
962 analogy, one would not expect window wipers to suddenly turn on and the horn to honk
963 several days after running out of gas.

964 Since the postmortem upregulation of genes occurred in both the zebrafish and the mouse
965 in our study, it is reasonable to suggest that other multicellular eukaryotes will display a
966 similar phenomenon. What does this phenomenon mean in the context of organismal
967 life? We conjecture that the highly ordered structure of an organism – evolved and
968 refined through natural selection and self-organizing processes – undergoes a
969 thermodynamically driven process of spontaneous disintegration through complex
970 pathways, which apparently involve the upregulation of genes and feedback loops. While
971 evolution played a role in pre-patterning of these pathways, it does not play any role in its
972 disintegration fate. One could argue that some of these pathways have evolved to favor
973 healing or "resuscitation" after severe injury. For example, the upregulation of
974 inflammation response genes indicate that a signal of infection or injury is sensed by the
975 still alive cells after death of the body. Alternatively, the upregulation may be due to fast
976 decay of some repressors of genes or whole pathways (see below). Hence, it will be of
977 interest to study this in more detail, since this could, for example, provide insights into
978 how to better preserve organs retrieved for transplantation.

Chemical automator – on the way down to equilibrium

980 As one would expect, a living system is a collection of chemical reactions linked together
981 by the chemicals participating in them. Having these reactions to depend on one another

982 to a certain extent, we conjecture that the observed upregulation of genes is due to
983 thermodynamic and kinetic controls that are encountered during organismal death. For
984 example, epigenetic regulatory genes that were upregulated included histone modification
985 genes (e.g., *Histh1l*) and genes interacting with chromatin (e.g., *Grwd1, Chd3, Yeats,*
986 *Jmjd1c*) (Fig 10). It is possible that the activation of these genes was responsible for the
987 unraveling of the nucleosomes, which enabled transcription factors and RNA
988 polymerases to transcribe developmental genes that have been previously silenced since
989 embryogenesis. The energy barrier in this example is the tightly wrapped nucleosomes
990 that previously did not allow access to developmental genes. Other energy or entropy
991 barriers could be nucleopores that allow the exchange of mRNA and other molecules
992 between the mitochondria and the cytosol (e.g., *Tpr, Tnpo1, Lrrc59*), or the ion/solute
993 protein channels (e.g., *Aralar2, Slc38a4*) that control intracellular ions that regulate
994 apoptotic pathways [194,195].

995 The upregulation of genes indicates new molecules were synthesized. Hence, there was
996 sufficient energy and resources (e.g., RNA polymerase, dNTPs) in dead organisms to
997 maintain gene transcription to 96 h (e.g., *Zfand4*, *Tox2*, and *Slc14a2*) in the zebrafish and
998 to 48 h (e.g., *Deg2, Ogfod1,* and *Ifitm1*) in the mouse. Gene transcription was apparently
999 not prevented due to a lack of energy or resources. Several genes exhibited apparent
1000 regulation by feedback loops in their transcriptional profiles (e.g., *Rbm45* and *Cdc42*
1001 genes in the mouse (Fig 8 and 9, respectively; Fig S3)). Hence, an underlying regulatory
1002 network appears to be still turning "on" and "off" genes in organismal death.

1003 **Interrupt the shutdown?**
1004 A living biological system is a product of natural selection and self-organizing processes
1005 [196]. Genes are transcribed and proteins translated in response to genetic and epigenetic
1006 regulatory networks that sustain life. In organismal death, we assumed most of the
1007 genetic and epigenetic regulatory networks operating in life would become disengaged
1008 from the rest of the organism. However, we found that "dead" organisms turn genes on
1009 and off in a non-random manner (Fig 2D and 2E). There is a range of times in which
1010 genes are upregulated and transcript abundances are maximized. While most genes are
1011 upregulated within 0.5 h postmortem (Fig 11), some are upregulated at 24 h and still
1012 others at 48 h. A similar pattern occurs with peak transcript abundances and the timing
1013 when upregulation is apparently stopped. These differences in timings and abundances
1014 suggest some sort of global regulation network is still operating in both organisms. What
1015 makes gene expression of life different from gene expression in death is that postmortem
1016 upregulation of genes offers no obvious benefit to an organism. We argue that self-
1017 organizing processes driven by thermodynamics are responsible for the postmortem
1018 upregulation of genes. We emphasize that such postmortem conditions could allow
1019 investigators to tease apart evolution from self-organizing processes that are typically
1020 entangled in life.

1021 Since our results show that the system has not reached equilibrium yet, it would be
1022 interesting to address the following question: *what would happen if we arrested the*
1023 *process of dying by providing nutrients and oxygen to tissues?* It might be possible for
1024 cells to revert back to life or take some interesting path to differentiating into something
1025 new or lose differentiation altogether, such as in cancer. We speculate that the recovering

1026 cells will likely depend on the postmortem time – at least when such potentially
1027 interesting effects might be seen.

Methodological validity

1029 The Gene Meter approach is pertinent to the quality of the microarray output obtained in
1030 this study because conventional DNA microarrays yield noisy data [197,198]. The Gene
1031 Meter approach determines the behavior of every microarray probe by calibration –
1032 which is analogous to calibrating a pH meter with buffers. Without calibration, the
1033 precision and accuracy of a meter is not known, nor can one know how well the
1034 experimental data fits to the calibration (i.e., R^2). In the Gene Meter approach, the
1035 response of a probe (i.e., its behavior in a dilution series) is fitted to either Freundlich or
1036 Langmuir adsorption model, probe-specific parameters are calculated. The "noisy" or
1037 "insensitive" probes are identified and removed from further analyses. Probes that
1038 sufficiently fit the model are retained and later used to calculate the abundance of a
1039 specific gene in a biological sample. The models take into consideration the non-linearity
1040 of the microarray signal and the calibrated probes do not require normalization
1041 procedures to compare biological samples. In contrast, conventional DNA microarray
1042 approaches are biased because different normalizations can yield up to 20 to 30%
1043 differences in the up- or down-regulation depending on the procedure selected [199-202].
1044 We recognize that next-generation-sequencing (NGS) approaches could have been used
1045 to monitor gene expression in this study. However, the same problems of normalization
1046 and reproducibility (mentioned above) are pertinent to NGS technology [203]. Hence,
1047 the Gene Meter approach is currently the most advantageous to study postmortem gene
1048 expression in a high throughput manner.

Practical implications

1050 The postmortem upregulation of genes in the mouse has relevance to transplantation
1051 research. We observed clear qualitative and quantitative differences between two organs
1052 (liver and brain) in the mouse in their degradation profiles (Fig 1). We also showed the
1053 upregulation of immunity, inflammation and cancer genes within 1 h of death (Fig 11). It
1054 would be interesting to explore if these differences are comparable to what occurs in
1055 humans, and we wonder how much of the transplant success could be attributed to
1056 differences in the synchronicity of postmortem expression profiles rather than
1057 immunosuppression agents [204,205]. Our study provides an alternative perspective to
1058 the fate of transplant recipients due to the upregulation of regulatory and response genes,
1059 after the sample has been harvested from the donor.

Conclusion

1061 This is the first study to demonstrate active, long-term expression of genes in organismal
1062 death that raises interesting questions relative to transplantology, inflammation, cancer,
1063 evolution, and molecular biology.

1064

Competing Interests

1066 The authors declare that they have no competing interests.

1067

Authors' contributions

1069 DT, RN, TDL and AEP designed the study. AEP, RN, TDL carried out the molecular
1070 genetic studies. BGL and AEP determined the statistically significant upregulated genes.
1071 SS and PAN annotated the genes. AEP and PAN conducted the statistical analyses and
1072 wrote the manuscript. All authors read and approved the final manuscript.

Acknowledgements

REFERENCES

1. Monod J. Genetic regulatory mechanisms in the synthesis of proteins. J Mol Biol. 1961;3: 318.

2. Zong WX, Thompson CB. Necrotic death as a cell fate. Genes Dev. 2006, 20: 1.

3. GalluzziL, Bravo-San Pedro JM, Kroemer G. Organelle-specific initiation of cell death. Nat Cell Biol. 2014;16: 728-736.

4. Ferriferri_2001 KF, Kroemer G. Organelle-specific initiation of cell death pathways. Nat Cell Biol. 2001;3: E255.

5. Syntichakisyntichaki_2002 P, Tavernarakis N. Death by necrosis. Uncontrollable catastrophe, or is there order behind the chaos? EMBO Rep. 2002;3: 604.

6. Pozhitkov AE, Noble PA, Bryk J, Tautz D. A revised design for microarray experiments to account for experimental noise and uncertainty of probe response. PLoS One. 2014;9: e91295.

7. Domazet-Loso T, Tautz D. Phylostratigraphic tracking of cancer genes suggests a link to the emergence of multicellularity in metazoa. BMC Biol. 2010;8: 66. doi: 10.1186/1741-7007-8-66.

8. Seear PJ, Sweeney GE. Stability of RNA isolated from post-mortem tissues of Atlantic salmon (Salmo salar L.). Fish Physiol Biochem. 2008;34: 19-24. doi: 10.1007/s10695-007-9141-x.

9. Bahar B, Monahan FJ, Moloney AP, Schmidt O, MacHugh DE, Sweeney T. Long-term stability of RNA in post-mortem bovine skeletal muscle, liver and subcutaneous adipose tissues. BMC Mol Biol. 2007;8: 108.

10. Inoue H, Kimura A, Tuji T. Degradation profile of mRNA in a dead rat body: basic semi-quantification study. Forensic Sci Int. 2002;130: 127-32.

11. Johnson SA, Morgan DG, Finch CE. Extensive postmortem stability of RNA from rat and human brain. J Neurosci Res. 1986;16: 267-80.

12. Catts VS, Catts SV, Fernandez HR, Taylor JM, Coulson EJ, Lutze-Mann LH. A microarray study of post-mortem mRNA degradation in mouse brain tissue. Brain Res Mol Brain Res. 2005;138: 164-77.

13. Heinrich M, Matt K, Lutz-Bonengel S, Schmidt U. Successful RNA extraction from various human postmortem tissues. Int J Legal Med. 2007;121: 136-42.

14. Neymotin, Athanasiadou R, Gresham D. Determination of in vivo RNA kinetics using RATE-seq. RNA. 2014;20: 1645.

15. Spilka R, Ernst C, Bergler H, Rainer J, Flechsig S, Vogetseder A, Lederer E, Benesch M, Brunner A, Geley S, Eger A, Bachmann F, Doppler W, Obrist P, Haybaeck J. eIF3a is over-expressed in urinary bladder cancer and influences its phenotype independent of translation initiation. Cell Oncol (Dordr). 2014;37: 253

1122 16. Bortolotti GR, Tella JL, Baos R, Marchant TA. Stress response during development
1123   predicts fitness in a wild, long lived vertebrate. Proc Natl Acad Sci USA. 2007;104:
1124   8880-4.

1125 17. Skaggs HS, Xing H, Wilkerson DC, Murphy LA, Hong Y, Mayhew CN, Sarge KD.
1126   HSF1-TPR interaction facilitates export of stress-induced HSP70 mRNA. J Biol
1127   Chem. 2007;282: 33902-7.

1128 18. Snow CJ, Paschal BM. Roles of the nucleoporin Tpr in cancer and aging. Adv Exp
1129   Med Biol. 2014;773: 309-22. doi: 10.1007/978-1-4899-8032-8_14.

1130 19. David-Watine B. Silencing nuclear pore protein Tpr elicits a senescent-like
1131   phenotype in cancer cells. PLoS One. 2011;6: e22423. doi:
1132   10.1371/journal.pone.0022423.

1133 20. Kadeba PI, Scammel JG, Cioffi DL. The chaperone heat shock protein 90 (Hsp90)
1134   participates in the endothelial store operated calcium entry heterocomplex. FASEB J.
1135   2013;27: 724.4

1136 21. Mayer MP, Bukau B. Hsp70 chaperones: cellular functions and molecular
1137   mechanism. Cell Mol Life Sci. 2005;62: 670-84.

1138 22. Jakobsson ME, Davydova E, Małecki J, Moen A, Falnes, PØ. Saccharomyces
1139   cerevisiae eukaryotic elongation factor 1A (eEF1A) is methylated at Lys-390 by a
1140   METTL21-like methyltransferase. PLos One 2015;
1141   doi:10.1371/journal.pone.0131426.t002.

1142 23. Höhfeld J, Hartl FU. Requirement of the chaperonin cofactor Hsp10 for protein
1143   sorting in yeast mitochondria. J Cell Biol/ 1994;126:305–315.

1144 24. Wu BJ, Morimoto RI. Transcription of the human hsp70 gene is induced by serum
1145   stimulation. Proc Natl Acad Sci USA. 1985;82: 6070-4.

1146 25. Ngr di A, Domoki F, Dgi R, Borda S, Pkski M, Szab A, Bari F. Up-regulation of
1147   cerebral carbonic anhydrase by anoxic stress in piglets. J Neurochem. 2003;85: 843-
1148   50.

1149 26. Lin KH, Kuo CH, Kuo WW, Ho TJ, Pai P, Chen WK, Pan LF, Wang CC, Padma VV,
1150   Huang CY. NFIL3 suppresses hypoxia-induced apoptotic cell death by targeting the
1151   insulin-like growth factor 2 receptor. J Cell Biochem. 2015;116: 1113-20. doi:
1152   10.1002/jcb.25067

1153 27. Zhang W, Zhang J, Kornuc M, Kwan K, Frank R, Nimer SD. Molecular cloning and
1154   characterization of NF-IL3A, a transcriptional activator of the human interleukin-3
1155   promoter. Mol Cell Biol. 1995;15: 6055-63.

1156 28. Smith TG, Robbins PA, Ratcliffe PJ. The human side of hypoxia-inducible factor. Br
1157   J Haematol. 2008, 141: 325-34. doi: 10.1111/j.1365-2141.2008.07029.x.

1158 29. Ino Y, Yamazaki-Itoh R, Oguro S, Shimada K, Kosuge T, Zavada J, Kanai Y,
1159   Hiraoka N. Arginase II expressed in cancer-associated fibroblasts indicates tissue
1160   hypoxia and predicts poor outcome in patients with pancreatic cancer. PLoS One.
1161   2013;8: e55146. doi: 10.1371/journal.pone.0055146.

30. Lafleur VN, Richard S, Richard DE. Transcriptional repression of hypoxia-inducible factor-1 (HIF-1) by the protein arginine methyltransferase PRMT1. Mol Biol Cell. 2014;25: 925-35. doi: 10.1091/mbc.E13-07-0423.

31. Devlin CM, Lahm T, Hubbard WC, Van Demark M, Wang KC, Wu X, Bielawska A, Obeid LM, Ivan M, Petrache I. Dihydroceramide-based response to hypoxia. J Biol Chem. 2011;286: 38069-78. doi: 10.1074/jbc.M111.297994.

32. Hannun YA, Obeid LM. Principles of bioactive lipid signalling: lessons from sphingolipids. Nat Rev Mol Cell Biol. 2008;9: 139-50. doi: 10.1038/nrm2329.

33. Mao C, Obeid LM. Ceramidases: regulators of cellular responses mediated by ceramide, sphingosine, and sphingosine-1-phosphate. Biochim Biophys Acta. 2008;1781: 424-34. doi: 10.1016/j.bbalip.2008.06.002.

34. Rhee SG, Chae HZ, Kim K. Peroxiredoxins: a historical overview and speculative preview of novel mechanisms and emerging concepts in cell signaling. Free Radic Biol Med. 2005;38: 1543-52.

35. Salzano S, Checconi P, Hanschmann EM, Lillig CH, Bowler LD, Chan P, Vaudry D, Mengozzi M, Coppo L, Sacre S, Atkuri KR, Sahaf B, Herzenberg LA, Herzenberg LA, Mullen L, Ghezzi P. Linkage of inflammation and oxidative stress via release of glutathionylated peroxiredoxin-2, which acts as a danger signal. Proc Natl Acad Sci USA. 2014;111: 12157-62. doi: 10.1073/pnas.1401712111.

36. Landau G, Ran A, Bercovich Z, Feldmesser E, Horn-Saban S, Korkotian E, Jacob-Hirsh J, Rechavi G, Ron D, Kahana C. Expression profiling and biochemical analysis suggest stress response as a potential mechanism inhibiting proliferation of polyamine-depleted cells. J Biol Chem. 2012; 287:35825-37. doi: 10.1074/jbc.M112.381335.

37. Fornace AJ Jr, Jackman J, Hollander MC, Hoffman-Liebermann B, Liebermann DA. Genotoxic-stress-response genes and growth-arrest genes. gadd, MyD, and other genes induced by treatments eliciting growth arrest. Ann N Y Acad Sci. 1992;663: 139-53.

38. Schmitz I. Gadd45 proteins in immunity. In: D.A. Liebermann and B. Hoffman (eds), Gadd45 Stress Sensor Genes, Advances in Experimental Medicine and Biology 793, Springer Science+Business Media New York 2013.

39. Lisowski P, Wieczorek M, Goscik J, Juszczak GR, Stankiewicz AM, Zwierzchowski L, Swiergiel AH. Effects of chronic stress on prefrontal cortex transcriptome in mice displaying different genetic backgrounds. J Mol Neurosci. 2013;50: 33-57. doi: 10.1007/s12031-012-9850-1.

40. Timpl P, Spanagel R, Sillaber I, Kresse A, Reul JM, Stalla GK, Blanquet V, Steckler T, Holsboer F, Wurst W. Impaired stress response and reduced anxiety in mice lacking a functional corticotropin-releasing hormone receptor 1. Nat Genet. 1998;19: 162-6.

41. Leikauf GD, Concel VJ, Bein K, Liu P, Berndt A, Martin TM, Ganguly K, Jang AS, Brant KA, Dopico RA Jr, Upadhyay S, Cario C, Di YP, Vuga LJ, Kostem E, Eskin E, You M, Kaminski N, Prows DR, Knoell DL, Fabisiak JP. Functional genomic

1204   assessment of phosgene-induced acute lung injury in mice. Am J Respir Cell Mol
1205   Biol. 2013;49: 368-83. doi: 10.1165/rcmb.2012-0337OC.

1206 42. Nice TJ, Deng W, Coscoy L, Raulet DH. Stress-regulated targeting of the NKG2D
1207   ligand Mult1 by a membrane-associated RING-CH family E3 ligase. J Immunol.
1208   2010;185: 5369-76. doi: 10.4049/jimmunol.1000247.

1209 43. Kokame K, Agarwala KL, Kato H, Miyata T. Herp, a new ubiquitin-like membrane
1210   protein induced by endoplasmic reticulum stress. J Biol Chem. 2000;275: 32846-53.

1211 44. Coates PJ, Nenutil R, McGregor A, Picksley SM, Crouch DH, Hall PA, Wright EG.
1212   Mammalian prohibitin proteins respond to mitochondrial stress and decrease during
1213   cellular senescence. Exp Cell Res. 2001; 265:262-73.

1214 45. Wehner KA, Schtz S, Sarnow P. OGFOD1, a novel modulator of eukaryotic
1215   translation initiation factor 2alpha phosphorylation and the cellular response to stress.
1216   Mol Cell Biol. 2010;30: 2006-16. doi: 10.1128/MCB.01350-09.

1217 46. Rock KL, Lai JJ, Kono H. Innate and adaptive immune responses to cell death.
1218   Immunol Rev. 2011;243: 191-205. doi: 10.1111/j.1600-065X.2011.01040.x.

1219 47. Crist SA, Elzey BD, Ahmann MT, Ratliff TL. Early growth response-1 (EGR-1) and
1220   nuclear factor of activated T cells (NFAT) cooperate to mediate CD40L expression in
1221   megakaryocytes and platelets. J Biol Chem. 2013;288: 33985-96. doi:
1222   10.1074/jbc.M113.511881.

1223 48. Li S, Miao T, Sebastian M, Bhullar P, Ghaffari E, Liu M, Symonds AL, Wang P. The
1224   transcription factors Egr2 and Egr3 are essential for the control of inflammation and
1225   antigen-induced proliferation of B and T cells. Immunity. 2012;37: 685-96. doi:
1226   10.1016/j.immuni.2012.08.001.

1227 49. Jayaraman P, Sada-Ovalle I, Nishimura T, Anderson AC, Kuchroo VK, Remold HG,
1228   Behar SM. IL-1β promotes antimicrobial immunity in macrophages by regulating
1229   TNFR signaling and caspase-3 activation. J Immunol. 2013;190: 4196-204. doi:
1230   10.4049/jimmunol.1202688.

1231 50. Hughes AL. Origin and diversification of the L-amino oxidase family in innate
1232   immune defenses of animals. Immunogenetics. 2010;62: 753-9. doi: 10.1007/s00251-
1233   010-0482-8.

1234 51. Ramirez-Carrozzi V, Sambandam A, Luis E, Lin Z, Jeet S, Lesch J, Hackney J, Kim
1235   J, Zhou M, Lai J, Modrusan Z, Sai T, Lee W, Xu M, Caplazi P, Diehl L, de Voss J,
1236   Balazs M, Gonzalez L Jr, Singh H, Ouyang W, Pappu R. IL-17C regulates the innate
1237   immune function of epithelial cells in an autocrine manner. Nat Immunol. 2011;12:
1238   1159-66 doi: 10.1038/ni.2156.

1239 52. Zuccolo J, Bau J, Childs SJ, Goss GG, Sensen CW, Deans JP. Phylogenetic analysis
1240   of the MS4A and TMEM176 gene families. PLoS One. 2010, 5: e9369. doi:
1241   10.1371/journal.pone.0009369.

1242 53. Allen A, Hutton DA, Pearson JP. The MUC2 gene product: a human intestinal mucin.
1243   Int J Biochem Cell Biol. 1998;30: 797-801.

1244   54. Michelucci A, Cordes T, Ghelfi J, Pailot A, Reiling N, Goldmann O, Binz T, Wegner
1245   A, Tallam A, Rausell A, Buttini M, Linster CL, Medina E, Balling R, Hiller K.
1246   Immune-responsive gene 1 protein links metabolism to immunity by catalyzing
1247   itaconic acid production. Proc Natl Acad Sci USA. 2013;110: 7820-5. doi:
1248   10.1073/pnas.1218599110.

1249   55. Honke N, Shaabani N, Cadeddu G, Sorg UR, Zhang DE, Trilling M, Klingel K,
1250   Sauter M, Kandolf R, Gailus N, van Rooijen N, Burkart C, Baldus SE, Grusdat M,
1251   Lhning M, Hengel H, Pfeffer K, Tanaka M, Hussinger D, Recher M, Lang PA, Lang
1252   KS. Enforced viral replication activates adaptive immunity and is essential for the
1253   control of a cytopathic virus. Nat Immunol. 2011;13: 51-7. doi: 10.1038/ni.2169.

1254   56. Martnez-Lpez M, Iborra S, Conde-Garrosa R, Sancho D. Batf3-dependent CD103+
1255   dendritic cells are major producers of IL-12 that drive local Th1 immunity against
1256   Leishmania major infection in mice. Eur J Immunol. 2015;45: 119-29. doi:
1257   10.1002/eji.201444651.

1258   57. Imai T, Baba M, Nishimura M, Kakizaki M, Takagi S, Yoshie O. The T cell-directed
1259   CC chemokine TARC is a highly specific biological ligand for CC chemokine
1260   receptor 4. J Biol Chem. 1997;272: 15036-42.

1261   58. Vong QP, Leung WH1, Houston J1, Li Y1, Rooney B1, Holladay M1, Oostendorp
1262   RA2, Leung W3. TOX2 regulates human natural killer cell development by
1263   controlling T-BET expression. Blood. 2014;124: 3905-13. doi: 10.1182/blood-2014-
1264   06-582965.

1265   59. Takaori A. Antiviral defense by APOBEC3 family proteins. Uirusu. 2005;55: 267-72.

1266   60. Arming S, Wipfler D, Mayr J, Merling A, Vilas U, Schauer R, Schwartz-Albiez R,
1267   Vlasak R. The human Cas1 protein: a sialic acid-specific O-acetyltransferase?
1268   Glycobiology. 2011;21: 553-64. doi: 10.1093/glycob/cwq153.

1269   61. Crocker PR, Paulson JC, Varki A. Siglecs and their roles in the immune system. Nat
1270   Rev Immunol. 2007;7: 255-66.

1271   62. Crocker PR, Varki A. Siglecs in the immune system. Immunology. 2001;103: 137-45.

1272   63. Shi WX, Chammas R, Varki NM, Powell L, Varki A. Sialic acid 9-O-acetylation on
1273   murine erythroleukemia cells affects complement activation, binding to I-type lectins,
1274   and tissue homing. J Biol Chem. 1996;271: 31526-32.

1275   64. Praper T, Sonnen A, Viero G, Kladnik A, Froelich CJ, Anderluh G, Dalla Serra M,
1276   Gilbert RJ. Human perforin employs different avenues to damage membranes. J Biol
1277   Chem. 2011;286: 2946-55. doi: 10.1074/jbc.M110.169417.

1278   65. Tschopp J, Masson D, Stanley KK. Structural/functional similarity between proteins
1279   involved in complement- and cytotoxic T-lymphocyte-mediated cytolysis. Nature.
1280   1986;322: 831-4.

1281   66. White SH, Wimley WC, Selsted ME. Structure, function, and membrane integration
1282   of defensins. Curr Opin Struct Biol. 1995;5: 521-7.

1283   67. Blanchong CA, Chung EK, Rupert KL, Yang Y, Yang Z, Zhou B, Moulds JM, Yu
1284   CY. Genetic, structural and functional diversities of human complement components

C4A and C4B and their mouse homologues, Slp and C4. Int Immunopharmacol. 2001;1: 365-92.

68. Chen L, Carico Z, Shih HY, Krangel MS. A discrete chromatin loop in the mouse Tcra-Tcrd locus shapes the TCRδ and TCRα repertoires. Nat Immunol. 2015;16: 1085-93. doi: 10.1038/ni.3232.

69. Grage-Griebenow E, Flad HD, Ernst M, Bzowska M, Skrzeczyska J, Pryjma J. Human MO subsets as defined by expression of CD64 and CD16 differ in phagocytic activity and generation of oxygen intermediates. Immunobiology. 2000;202: 42-50.

70. Al-Banna NA, Vaci M, Slauenwhite D, Johnston B, Issekutz TB. CCR4 and CXCR3 play different roles in the migration of T cells to inflammation in skin, arthritic joints, and lymph nodes. Eur J Immunol. 2014;44: 1633-43. doi: 10.1002/eji.201343995. Epub 2014 Apr 23.

71. Ikutani M, Yanagibashi T, Ogasawara M, Tsuneyama K, Yamamoto S, Hattori Y, Kouro T, Itakura A, Nagai Y, Takaki S, Takatsu K. Identification of innate IL-5-producing cells and their role in lung eosinophil regulation and antitumor immunity. J Immunol. 2012;188: 703-13. doi: 10.4049/jimmunol.1101270. Epub 2011 Dec 14.

72. Lillard JW Jr, Boyaka PN, Taub DD, McGhee JR. RANTES potentiates antigen-specific mucosal immune responses. J Immunol. 2001;166: 162-9.

73. Kawasaki N, Rademacher C, Paulson JC. CD22 regulates adaptive and innate immune responses of B cells. J Innate Immun. 2011;3: 411-9. doi: 10.1159/000322375.

74. Liu H, Thaker YR, Stagg L, Schneider H, Ladbury JE, Rudd CE. SLP-76 sterile α motif (SAM) and individual H5 α helix mediate oligomer formation for microclusters and T-cell activation. J Biol Chem. 2013;288: 29539-49. doi: 10.1074/jbc.M112.424846.

75. Feeley EM, Sims JS, John SP, Chin CR, Pertel T, Chen LM, Gaiha GD, Ryan BJ, Donis RO, Elledge SJ, Brass AL. IFITM3 inhibits influenza A virus infection by preventing cytosolic entry. PLoS Pathog. 2011;7: e1002337. doi: 10.1371/journal.ppat.1002337.

76. Saben J, Zhong Y, Gomez-Acevedo H, Thakali KM, Borengasser SJ, Andres A, Shankar K. Early growth response protein-1 mediates lipotoxicity-associated placental inflammation: role in maternal obesity. Am J Physiol Endocrinol Metab. 2013;305: e1-14. doi: 10.1152/ajpendo.00076.2013.

77. Ren K, Torres R. Role of interleukin-1beta during pain and inflammation. Brain Res Rev. 2009;60: 57-64. doi: 10.1016/j.brainresrev.2008.12.020.

78. Chen GY, Nuñez G. Sterile inflammation: sensing and reacting to damage. Nat Rev Immunol. 2010;10: 826-37. doi: 10.1038/nri2873.

79. Sedger LM, McDermott MF. TNF and TNF-receptors: From mediators of cell death and inflammation to therapeutic giants - past, present and future. Cytokine Growth Factor Rev. 2014;25: 453-72. doi: 10.1016/j.cytogfr.2014.07.016.

80. Lee TS, Chau LY. Heme oxygenase-1 mediates the anti-inflammatory effect of interleukin-10 in mice. Nat Med. 2002;8: 240-6.

81. Piantadosi CA, Withers CM, Bartz RR, MacGarvey NC, Fu P, Sweeney TE, Welty-Wolf KE, Suliman HB. Heme oxygenase-1 couples activation of mitochondrial biogenesis to anti-inflammatory cytokine expression. J Biol Chem. 2011;286: 16374-85. doi: 10.1074/jbc.M110.207738.

82. Guo Y, Zhang W, Giroux C, Cai Y, Ekambaram P, Dilly AK, Hsu A, Zhou S, Maddipati KR, Liu J, Joshi S, Tucker SC, Lee MJ, Honn KV. Identification of the orphan G protein-coupled receptor GPR31 as a receptor for 12-(S)-hydroxyeicosatetraenoic acid. J Biol Chem. 2011;286: 33832-40. doi: 10.1074/jbc.M110.216564.

83. Bickel M. The role of interleukin-8 in inflammation and mechanisms of regulation. J Periodontol. 1993;64: 456-60.

84. Alcock J, Franklin ML, Kuzawa CW. Nutrient signaling: evolutionary origins of the immune-modulating effects of dietary fat. Q Rev Biol 2012;87: 187-223.

85. Pearson G, Robinson F, Beers Gibson T, Xu BE, Karandikar M, Berman K, Cobb MH. Mitogen-activated protein (MAP) kinase pathways: regulation and physiological functions. Endocr Rev. 2001;22: 153-83.

86. Tsatsanis C, Androulidaki A, Dermitzaki E, Gravanis A, Margioris AN. Corticotropin releasing factor receptor 1 (CRF1) and CRF2 agonists exert an anti-inflammatory effect during the early phase of inflammation suppressing LPS-induced TNF-alpha release from macrophages via induction of COX-2 and PGE2. J Cell Physiol. 2007;210: 774-83.

87. Frugier T, Morganti-Kossmann MC, O'Reilly D, McLean CA. In situ detection of inflammatory mediators in post mortem human brain tissue after traumatic injury. J Neurotrauma. 2010;27: 497-507. doi: 10.1089/neu.2009.1120.

88. Sawant DV, Sehra S, Nguyen ET, Jadhav R, Englert K, Shinnakasu R, Hangoc G, Broxmeyer HE, Nakayama T, Perumal NB, Kaplan MH, Dent AL. Bcl6 controls the Th2 inflammatory activity of regulatory T cells by repressing Gata3 function. J Immunol. 2012;189: 4759-69. doi: 10.4049/jimmunol.1201794.

89. Correa-Costa M, Andrade-Oliveira V, Braga TT, Castoldi A, Aguiar CF, Origassa CS2, Rodas AC, Hiyane MI, Malheiros DM, Rios FJ, Jancar S, Cmara NO. Activation of platelet-activating factor receptor exacerbates renal inflammation and promotes fibrosis. Lab Invest. 2014;94: 455-66. doi: 10.1038/labinvest.2013.155.

90. Watson RP, Lilley E, Panesar M, Bhalay G, Langridge S, Tian SS, McClenaghan C, Ropenga A, Zeng F, Nash MS. Increased prokineticin 2 expression in gut inflammation: role in visceral pain and intestinal ion transport. Neurogastroenterol Motil. 2012;24: 65-75 doi: 10.1111/j.1365-2982.2011.01804.x.

91. Pavlov VA, Wang H, Czura CJ, Friedman SG, Tracey KJ. The cholinergic anti-inflammatory pathway: a missing link in neuroimmunomodulation. Mol Med. 2003;9: 125-34.

1366 92. Lerdrup M, Holmberg C, Dietrich N, Shaulian E, Herdegen T, Jttel M, Kallunki T.
1367   Depletion of the AP-1 repressor JDP2 induces cell death similar to apoptosis.
1368   Biochim Biophys Acta. 2005;1745: 29-37.

1369 93. Hu W, Xu R, Sun W, Szulc ZM, Bielawski J, Obeid LM, Mao C. Alkaline
1370   ceramidase 3 (ACER3) hydrolyzes unsaturated long-chain ceramides, and its down-
1371   regulation inhibits both cell proliferation and apoptosis. J Biol Chem. 2010;285:
1372   7964-76. doi: 10.1074/jbc.M109.063586.

1373 94. Preston GA, Lyon TT, Yin Y, Lang JE, Solomon G, Annab L, Srinivasan DG,
1374   Alcorta DA, Barrett JC. Induction of apoptosis by c-Fos protein. Mol Cell Biol.
1375   1996;16: 211-8.

1376 95. Adrain C, Creagh EM, Martin SJ. Apoptosis-associated release of Smac/DIABLO
1377   from mitochondria requires active caspases and is blocked by Bcl-2. EMBO J.
1378   2001;20: 6627-36.

1379 96. McNeish IA, Lopes R, Bell SJ, McKay TR, Fernandez M, Lockley M, Wheatley SP,
1380   Lemoine NR. Survivin interacts with Smac/DIABLO in ovarian carcinoma cells but
1381   is redundant in Smac-mediated apoptosis. Exp Cell Res. 2005;302: 69-82.

1382 97. Zhao F, Wang Q. The protective effect of peroxiredoxin II on oxidative stress
1383   induced apoptosis in pancreatic β-cells. Cell Biosci. 2012;2: 22. doi: 10.1186/2045-
1384   3701-2-22.

1385 98. Wu X, Hernandez-Enriquez B, Banas M, Xu R, Sesti F. Molecular mechanisms
1386   underlying the apoptotic effect of KCNB1 K+ channel oxidation. J Biol Chem.
1387   2013;288: 4128-34. doi: 10.1074/jbc.M112.440933.

1388 99. Tang D, Lahti JM, Kidd VJ. Caspase-8 activation and bid cleavage contribute to
1389   MCF7 cellular execution in a caspase-3-dependent manner during staurosporine-
1390   mediated apoptosis. J Biol Chem. 2000;275: 9303-7.

1391 100.   Chinnadurai G, Vijayalingam S, Rashmi R. BIK, the founding member of the
1392   BH3-only family proteins: mechanisms of cell death and role in cancer and
1393   pathogenic processes. Oncogene. 2008;27: S20-9. doi: 10.1038/onc.2009.40.

1394 101.   Iwasa H, Kudo T, Maimaiti S, Ikeda M, Maruyama J, Nakagawa K, Hata Y. The
1395   RASSF6 tumor suppressor protein regulates apoptosis and the cell cycle via MDM2
1396   protein and p53 protein. J Biol Chem. 2013;288:30320-9. doi:
1397   10.1074/jbc.M113.507384.

1398 102.   Liu X, Dong C, Jiang Z, Wu WK, Chan MT, Zhang J, Li H, Qin K, Sun X.
1399   MicroRNA-10b downregulation mediates acute rejection of renal allografts by
1400   derepressing BCL2L11. Exp Cell Res. 2015;333: 155-63. doi:
1401   10.1016/j.yexcr.2015.01.018.

1402 103.   Sayed M, Pelech S, Wong C, Marotta A, Salh B. Protein kinase CK2 is involved
1403   in G2 arrest and apoptosis following spindle damage in epithelial cells. Oncogene.
1404   2001;20: 6994-7005.

1405 104.   Maddigan A, Truitt L, Arsenault R, Freywald T, Allonby O, Dean J, Narendran
1406   A, Xiang J, Weng A, Napper S, Freywald A. EphB receptors trigger Akt activation

and suppress Fas receptor-induced apoptosis in malignant T lymphocytes. J Immunol. 2011;187: 5983-94. doi: 10.4049/jimmunol.1003482.

105.   Okamoto S, Krainc D, Sherman K, Lipton SA. Antiapoptotic role of the p38 mitogen-activated protein kinase-myocyte enhancer factor 2 transcription factor pathway during neuronal differentiation. Proc Natl Acad Sci USA. 2000;97: 7561-6.

106.   Chiorazzi M, Rui L, Yang Y, Ceribelli M, Tishbi N, Maurer CW, Ranuncolo SM, Zhao H, Xu W, Chan WC, Jaffe ES, Gascoyne RD, Campo E, Rosenwald A, Ott G, Delabie J, Rimsza LM, Shaham S, Staudt LM. Related F-box proteins control cell death in Caenorhabditis elegans and human lymphoma. Proc Natl Acad Sci USA. 2013;110: 3943-8. doi: 10.1073/pnas.1217271110.

107.   Bloch DB, Nakajima A, Gulick T, Chiche JD, Orth D, de La Monte SM, Bloch KD. Sp110 localizes to the PML-Sp100 nuclear body and may function as a nuclear hormone receptor transcriptional coactivator. Mol Cell Biol. 2000;20: 6138-46.

108.   Bengoechea-Alonso MT, Ericsson J. Tumor suppressor Fbxw7 regulates TGFβ signaling by targeting TGIF1 for degradation. Oncogene. 2010;29: 5322-8. doi: 10.1038/onc.2010.278. Epub 2010 Jul 12.

109.   Ma Y, Wang B, Li W, Ying G, Fu L, Niu R, Gu F. Reduction of intersectin1-s induced apoptosis of human glioblastoma cells. Brain Res. 2010;1351: 222-8. doi: 10.1016/j.brainres.2010.05.028.

110.   Gnesutta N, Qu J, Minden A. The serine/threonine kinase PAK4 prevents caspase activation and protects cells from apoptosis. J Biol Chem. 2001;276: 14414-9.

111.   Markovich D. Physiological roles and regulation of mammalian sulfate transporters. Physiol Rev. 2001;81: 1499-533.

112.   Guasti L, Crociani O, Redaelli E, Pillozzi S, Polvani S, Masselli M, Mello T, Galli A, Amedei A, Wymore RS, Wanke E, Arcangeli A. Identification of a posttranslational mechanism for the regulation of hERG1 K+ channel expression and hERG1 current density in tumor cells. Mol Cell Biol. 2008;28: 5043-60. doi: 10.1128/MCB.00304-08.

113.   Bremser M, Nickel W, Schweikert M, Ravazzola M, Amherdt M, Hughes CA, Sllner TH, Rothman JE, Wieland FT. Coupling of coat assembly and vesicle budding to packaging of putative cargo receptors. Cell. 1999;96: 495-506.

114.   Zhen Y, Srensen V, Skjerpen CS, Haugsten EM, Jin Y, Wlchli S, Olsnes S, Wiedlocha A. Nuclear import of exogenous FGF1 requires the ER-protein LRRC59 and the importins Kpnα1 and Kpnβ1. Traffic. 2012;13: 650-64. doi: 10.1111/j.1600-0854.2012.01341.x.

115.   Bangs P, Burke B, Powers C, Craig R, Purohit A, Doxsey S. Functional analysis of Tpr: identification of nuclear pore complex association and nuclear localization domains and a role in mRNA export. J Cell Biol. 1998;143: 1801-12.

116.   Nakielny S, Siomi MC, Siomi H, Michael WM, Pollard V, Dreyfuss G. Transportin: nuclear transport receptor of a novel nuclear protein import pathway. Exp Cell Res. 1996;229: 261-6.

1448 117.   Chi NC, Adam EJ, Adam SA. Sequence and characterization of cytoplasmic
1449   nuclear protein import factor p97. J Cell Biol. 1995;130: 265-74.

1450 118.   Tang BL, Low DY, Tan AE, Hong W. Syntaxin 10: a member of the syntaxin
1451   family localized to the trans-Golgi network. Biochem Biophys Res Commun.
1452   1998;242: 345-50.

1453 119.   Chen G. Biochemical properties of urea transporters. Subcell Biochem. 2014;73:
1454   109-26. doi: 10.1007/978-94-017-9343-8_7. PMID: 25298341

1455 120.   Palmieri L, Pardo B, Lasorsa FM, del Arco A, Kobayashi K, Iijima M, Runswick
1456   MJ, Walker JE, Saheki T, Satrstegui J, Palmieri F. Citrin and aralar1 are Ca(2+)-
1457   stimulated aspartate/glutamate transporters in mitochondria. EMBO J. 2001;20: 5060-
1458   9.

1459 121.   Hatanaka T, Huang W, Ling R, Prasad PD, Sugawara M, Leibach FH, Ganapathy
1460   V. Evidence for the transport of neutral as well as cationic amino acids by ATA3, a
1461   novel and liver-specific subtype of amino acid transport system A. Biochim Biophys
1462   Acta. 2001;1510: 10-7.

1463 122.   Conchon S, Cao X, Barlowe C, Pelham HR. Got1p and Sft2p: membrane proteins
1464   involved in traffic to the Golgi complex. EMBO J. 1999;18: 3934-46.

1465 123.   Hautbergue GM, Hung ML, Walsh MJ, Snijders AP, Chang CT, Jones R, Ponting
1466   CP, Dickman MJ, Wilson SA. UIF, a New mRNA export adaptor that works together
1467   with REF/ALY, requires FACT for recruitment to mRNA. Curr Biol. 2009;19: 1918-
1468   24. doi: 10.1016/j.cub.2009.09.041.

1469 124.   Grempler R, Augustin R, Froehner S, Hildebrandt T, Simon E, Mark M,
1470   Eickelmann P. Functional characterisation of human SGLT-5 as a novel kidney-
1471   specific sodium-dependent sugar transporter. FEBS Lett. 2012;586: 248-53. doi:
1472   10.1016/j.febslet.2011.12.027.

1473 125.   Dietmeier K, Hönlinger A, Bömer U, Dekker PJ, Eckerskorn C, Lottspeich F,
1474   Kübrich M, Pfanner N. Tom5 functionally links mitochondrial preprotein receptors to
1475   the general import pore. Nature. 1997;388: 195-200.

1476 126.   Annilo T, Shulenin S, Chen ZQ, Arnould I, Prades C, Lemoine C, Maintoux-
1477   Larois C, Devaud C, Dean M, Denfle P, Rosier M. Identification and characterization
1478   of a novel ABCA subfamily member, ABCA12, located in the lamellar ichthyosis
1479   region on 2q34. Cytogenet Genome Res. 2002;98: 169-76.

1480 127.   Moraes LA, Piqueras L, Bishop-Bailey D. Peroxisome proliferator-activated
1481   receptors and inflammation. Pharmacol Ther. 2006;110: 371-85.

1482 128.   Allikmets R, Gerrard B, Hutchinson A, Dean M. Characterization of the human
1483   ABC superfamily: isolation and mapping of 21 new genes using the expressed
1484   sequence tags database. Hum Mol Genet. 1996;5: 1649-55.

1485 129.   Chew CS, Parente JA Jr, Chen X, Chaponnier C, Cameron RS. The LIM and SH3
1486   domain-containing protein, lasp-1, may link the cAMP signaling pathway with
1487   dynamic membrane restructuring activities in ion transporting epithelia. J Cell Sci.
1488   2000;113: 2035-45.

1489 130. Phillips-Krawczak CA, Singla A, Starokadomskyy P, Deng Z, Osborne DG, Li H,
1490   Dick CJ, Gomez TS, Koenecke M, Zhang JS, Dai H, Sifuentes-Dominguez L2, Geng
1491   LN, Kaufmann SH, Hein MY, Wallis M, McGaughran J, Gecz J, Sluis Bv, Billadeau
1492   DD, Burstein E. COMMD1 is linked to the WASH complex and regulates endosomal
1493   trafficking of the copper transporter ATP7A. Mol Biol Cell. 2015;26: 91-103. doi:
1494   10.1091/mbc.E14-06-1073.

1495 131. Tyson JR, Stirling CJ. LHS1 and SIL1 provide a lumenal function that is essential
1496   for protein translocation into the endoplasmic reticulum. EMBO J. 2000;19: 6440-52.

1497 132. Sirrenberg C, Bauer MF, Guiard B, Neupert W, Brunner M. Import of carrier
1498   proteins into the mitochondrial inner membrane mediated by Tim22. Nature.
1499   1996;384: 582-5.

1500 133. Rubino M, Miaczynska M, Lipp R, Zerial M. Selective membrane recruitment of
1501   EEA1 suggests a role in directional transport of clathrin-coated vesicles to early
1502   endosomes. J Biol Chem. 2000;275: 3745-8.

1503 134. Zhu XR, Netzer R, Bhlke K, Liu Q, Pongs O. Structural and functional
1504   characterization of Kv6.2 a new gamma-subunit of voltage-gated potassium channel.
1505   Receptors Channels. 1999;6: 337-50.

1506 135. Toyama R, Kobayashi M, Tomita T, Dawid IB. Expression of LIM-domain
1507   binding protein (ldb) genes during zebrafish embryogenesis. Mech Dev. 1998;71:
1508   197-200.

1509 136. Kida YS, Sato T, Miyasaka KY, Suto A, Ogura T. Daam1 regulates the
1510   endocytosis of EphB during the convergent extension of the zebrafish notochord.
1511   Proc Natl Acad Sci USA. 2007;104: 6708-13.

1512 137. Gilpin BJ, Loechel F, Mattei MG, Engvall E, Albrechtsen R, Wewer UM. A
1513   novel, secreted form of human ADAM 12 (meltrin alpha) provokes myogenesis in
1514   vivo. J Biol Chem. 1998;273: 157-66.

1515 138. Sano K, Inohaya K, Kawaguchi M, Yoshizaki N, Iuchi I, Yasumasu S.
1516   Purification and characterization of zebrafish hatching enzyme - an evolutionary
1517   aspect of the mechanism of egg envelope digestion. FEBS J. 2008;275: 5934-46. doi:
1518   10.1111/j.1742-4658.2008.06722.x.

1519 139. Hofmeister-Brix A, Kollmann K, Langer S, Schultz J, Lenzen S, Baltrusch S.
1520   Identification of the ubiquitin-like domain of midnolin as a new glucokinase
1521   interaction partner. J Biol Chem. 2013;288: 35824-39. doi:
1522   10.1074/jbc.M113.526632.

1523 140. Tsukahara M, Suemori H, Noguchi S, Ji ZS, Tsunoo H. Novel nucleolar protein,
1524   midnolin, is expressed in the mesencephalon during mouse development. Gene.
1525   2000;254: 45-55.

1526 141. Hong SK, Dawid IB. FGF-dependent left-right asymmetry patterning in zebrafish
1527   is mediated by Ier2 and Fibp1. Proc Natl Acad Sci USA. 2009;106: 2230-5. doi:
1528   10.1073/pnas.0812880106.

1529 142.   Kwong RW, Perry SF. The tight junction protein claudin-b regulates epithelial
1530   permeability and sodium handling in larval zebrafish, Danio rerio. Am J Physiol
1531   Regul Integr Comp Physiol 2013;304: R504-13. doi: 10.1152/ajpregu.00385.2012.

1532 143.   Ing T, Aoki Y. Expression of RGS2, RGS4 and RGS7 in the developing postnatal
1533   brain. Eur J Neurosci. 2002;15: 929-36.

1534 144.   Wu T, Patel H, Mukai S, Melino C, Garg R, Ni X, Chang J, Peng C. Activin,
1535   inhibin, and follistatin in zebrafish ovary: expression and role in oocyte maturation.
1536   Biol Reprod. 2000;62: 1585-92.

1537 145.   Malinauskas T, Aricescu AR, Lu W, Siebold C, Jones EY. Modular mechanism
1538   of Wnt signaling inhibition by Wnt inhibitory factor 1. Nat Struct Mol Biol. 2011;18:
1539   886-93. doi: 10.1038/nsmb.2081.

1540 146.   Zagon IS, Wu Y, McLaughlin PJ. Opioid growth factor and organ development in
1541   rat and human embryos. Brain Res. 1999;839: 313-22.

1542 147.   Takano A, Zochi R, Hibi M, Terashima T, Katsuyama Y. Expression of
1543   strawberry notch family genes during zebrafish embryogenesis. Dev Dyn. 2010;239:
1544   1789-96. doi: 10.1002/dvdy.22287.

1545 148.   Pierani A, Moran-Rivard L, Sunshine MJ, Littman DR, Goulding M, Jessell TM.
1546   Control of interneuron fate in the developing spinal cord by the progenitor
1547   homeodomain protein Dbx1. Neuron. 2001;29: 367-84.

1548 149.   Buonamici S, Chakraborty S, Senyuk V, Nucifora G. The role of EVI1 in normal
1549   and leukemic cells. Blood Cells Mol Dis. 2003;31: 206-12.

1550 150.   Litwack ED, Babey R, Buser R, Gesemann M, O'Leary DD. Identification and
1551   characterization of two novel brain-derived immunoglobulin superfamily members
1552   with a unique structural organization. Mol Cell Neurosci. 2004;25: 263-74.

1553 151.   Gazit R, Mandal PK, Ebina W, Ben-Zvi A, Nombela-Arrieta C, Silberstein LE,
1554   Rossi DJ. Fgd5 identifies hematopoietic stem cells in the murine bone marrow. J Exp
1555   Med. 2014; 211: 1315-31. doi: 10.1084/jem.20130428.

1556 152.   Zhang J, Tomasini AJ, Mayer AN. RBM19 is essential for preimplantation
1557   development in the mouse. BMC Dev Biol. 2008;8: 115. doi: 10.1186/1471-213X-8-
1558   115.

1559 153.   Tang K, Xie X, Park JI, Jamrich M, Tsai S, Tsai MJ. COUP-TFs regulate eye
1560   development by controlling factors essential for optic vesicle morphogenesis.
1561   Development. 2010;137: 725-34. doi: 10.1242/dev.040568.

1562 154.   Zhang P, Bennoun M, Gogard C, Bossard P, Leclerc I, Kahn A, Vasseur-Cognet
1563   M. Expression of COUP-TFII in metabolic tissues during development. Mech Dev.
1564   2002;119: 109-14.

1565 155.   Coumailleau P, Duprez D. Sim1 and Sim2 expression during chick and mouse
1566   limb development. Int J Dev Biol. 2009;53: 149-57. doi: 10.1387/ijdb.082659pc.

1567 156.   Kondou H, Kawai M, Tachikawa K, Kimoto A, Yamagata M, Koinuma T,
1568   Yamazaki M, Nakayama M, Mushiake S, Ozono K, Michigami T. Sodium-coupled

1569   neutral amino acid transporter 4 functions as a regulator of protein synthesis during
1570   liver development. Hepatol Res. 2013;43: 1211-23. doi: 10.1111/hepr.12069.

1571   157.   Li Z, Lai G, Deng L, Han Y, Zheng D, Song W. Association of SLC38A4 and
1572   system A with abnormal fetal birth weight. Exp Ther Med. 2012;3: 309-313.

1573   158.   Tiberi L, van den Ameele J, Dimidschstein J, Piccirilli J, Gall D, Herpoel A,
1574   Bilheu A, Bonnefont J, Iacovino M, Kyba M, Bouschet T, Vanderhaeghen P. BCL6
1575   controls neurogenesis through Sirt1-dependent epigenetic repression of selective
1576   Notch targets. Nat Neurosci. 2012;15: 1627-35. doi: 10.1038/nn.3264.

1577   159.   Matsuoka RL, Sun LO, Katayama K, Yoshida Y, Kolodkin AL. Sema6B,
1578   Sema6C, and Sema6D expression and function during mammalian retinal
1579   development. PLoS One. 2013;8: e63207. doi: 10.1371/journal.pone.0063207.

1580   160.   Tamada H, Sakashita E, Shimazaki K, Ueno E, Hamamoto T, Kagawa Y, Endo H.
1581   cDNA cloning and characterization of Drb1, a new member of RRM-type neural
1582   RNA-binding protein. Biochem Biophys Res Commun. 2002;297: 96-104.

1583   161.   Rempel RE, Saenz-Robles MT, Storms R, Morham S, Ishida S, Engel A, Jakoi L,
1584   Melhem MF, Pipas JM, Smith C, Nevins JR. Loss of E2F4 activity leads to abnormal
1585   development of multiple cellular lineages. Mol Cell. 2000;6: 293-306.

1586   162.   Miyares RL, Stein C, Renisch B, Anderson JL, Hammerschmidt M, Farber SA.
1587   Long-chain Acyl-CoA synthetase 4A regulates Smad activity and dorsoventral
1588   patterning in the zebrafish embryo. Dev Cell. 2013;27: 635-47. doi:
1589   10.1016/j.devcel.2013.11.011.

1590   163.   Louryan S, Biermans J, Flemal F. Nerve growth factor in the developing
1591   craniofacial region of the mouse embryo. Eur J Morphol. 1995;33: 415-9.

1592   164.   Ko JA, Gondo T, Inagaki S, Inui M. Requirement of the transmembrane
1593   semaphorin Sema4C for myogenic differentiation. FEBS Lett. 2005;579: 2236-42.

1594   165.   Wu H, Fan J, Zhu L, Liu S, Wu Y, Zhao T, Wu Y, Ding X, Fan W, Fan M.
1595   Sema4C expression in neural stem/progenitor cells and in adult neurogenesis induced
1596   by cerebral ischemia. J Mol Neurosci. 2009;39: 27-39. doi: 10.1007/s12031-009-
1597   9177-8.

1598   166.   Pathirage NA, Cocquebert M, Sadovsky Y, Abumaree M, Manuelpillai U, Borg
1599   A, Keogh RJ, Brennecke SP, Evain-Brion D, Fournier T, Kalionis B, Murthi P.
1600   Homeobox gene transforming growth factor β-induced factor-1 (TGIF-1) is a
1601   regulator of villous trophoblast differentiation and its expression is increased in
1602   human idiopathic fetal growth restriction. Mol Hum Reprod. 2013;19: 665-75. doi:
1603   10.1093/molehr/gat042.

1604   167.   Heger S, Mastronardi C, Dissen GA, Lomniczi A, Cabrera R, Roth CL, Jung H,
1605   Galimi F, Sippell W, Ojeda SR. Enhanced at puberty 1 (EAP1) is a new
1606   transcriptional regulator of the female neuroendocrine reproductive axis. J Clin
1607   Invest. 2007;117: 2145-54.

1608   168.   Miao H, Strebhardt K, Pasquale EB, Shen TL, Guan JL, Wang B. Inhibition of
1609   integrin-mediated cell adhesion but not directional cell migration requires catalytic

1610 activity of EphB3 receptor tyrosine kinase. Role of Rho family small GTPases. J Biol
1611 Chem. 2005;280: 923-32.

1612 169. Vogel T, Boettger-Tong H, Nanda I, Dechend F, Agulnik AI, Bishop CE, Schmid
1613 M, Schmidtke J. A murine TSPY. Chromosome Res. 1998;6: 35-40.

1614 170. Janesick A, Shiotsugu J, Taketani M, Blumberg B. RIPPLY3 is a retinoic acid-
1615 inducible repressor required for setting the borders of the pre-placodal ectoderm.
1616 Development. 2012;139: 1213-24. doi: 10.1242/dev.071456.

1617 171. Zhou L, Zhang Z, Zheng Y, Zhu Y, Wei Z, Xu H, Tang Q, Kong X, Hu L.
1618 SKAP2, a novel target of HSF4b, associates with NCK2/F-actin at membrane ruffles
1619 and regulates actin reorganization in lens cell. J Cell Mol Med. 2011;15: 783-95. doi:
1620 10.1111/j.1582-4934.2010.01048.x.

1621 172. Wittschieben J, Shivji MK, Lalani E, Jacobs MA, Marini F, Gearhart PJ,
1622 Rosewell I, Stamp G, Wood RD. Disruption of the developmentally regulated Rev3l
1623 gene causes embryonic lethality. Curr Biol. 2000;10: 1217-20.

1624 173. Selvaraj A, Prywes R. Megakaryoblastic leukemia-1/2, a transcriptional co-
1625 activator of serum response factor, is required for skeletal myogenic differentiation. J
1626 Biol Chem. 2003;278: 41977-87.

1627 174. O'Shaughnessy RF, Welti JC, Sully K, Byrne C. Akt-dependent Pp2a activity is
1628 required for epidermal barrier formation during late embryonic development.
1629 Development. 2009;136: 3423-31. doi: 10.1242/dev.037010.

1630 175. Jaenisch R, Bird A. Epigenetic regulation of gene expression: how the genome
1631 integrates intrinsic and environmental signals. Nat Genet. 2003;33: 245-54.

1632 176. Gräff J, Kim D, Dobbin MM, Tsai LH. Epigenetic regulation of gene expression in
1633 physiological and pathological brain processes. Physiol Rev. 2011; 91: 603-49. doi:
1634 10.1152/physrev.00012.2010.

1635 177. Pan J, Jin C, Murata T, Yokoyama KK. Histone modification activities of JDP2
1636 associated with retinoic acid-induced differentiation of F9 cells. Nucleic Acids
1637 Symp Ser (Oxf). 2004;48: 189-90.

1638 178. Bowen NJ, Fujita N, Kajita M, Wade PA. Mi-2/NuRD: multiple complexes for
1639 many purposes. Biochim Biophys Acta. 2004;1677: 52-7.

1640 179. Sugimoto N, Maehara K, Yoshida K, Yasukouchi S, Osano S, Watanabe S, Aizawa
1641 M, Yugawa T, Kiyono T, Kurumizaka H, Ohkawa Y, Fujita M. Cdt1-binding
1642 protein GRWD1 is a novel histone-binding protein that facilitates MCM loading
1643 through its influence on chromatin architecture. Nucleic Acids Res. 2015;43: 5898-
1644 911. doi: 10.1093/nar/gkv509.

1645 180. Mariño-Ramírez L1, Kann MG, Shoemaker BA, Landsman D. Histone structure
1646 and nucleosome stability. Expert Rev Proteomics. 2005;2: 719-29.

1647 181. Yap KL, Li S, Muñoz-Cabello AM, Raguz S, Zeng L, Mujtaba S, Gil J, Walsh MJ,
1648 Zhou MM. Molecular interplay of the noncoding RNA ANRIL and methylated
1649 histone H3 lysine 27 by polycomb CBX7 in transcriptional silencing of INK4a.
1650 Mol Cell. 2010;38: 662-74. doi: 10.1016/j.molcel.2010.03.021.

182. Ikegamii K, Horigome D, Mukai M, Livnat I, MacGregor GR, Setou M. TTLL10 is a protein polyglycylase that can modify nucleosome assembly protein 1. FEBS Lett. 2008;582: 1129-34. doi: 10.1016/j.febslet.2008.02.079.

183. Marzluff WF, Gongidi P, Woods KR, Jin J, Maltais LJ. The human and mouse replication-dependent histone genes. Genomics. 2002;80: 487-98.

184. Li Y, Wen H, Xi Y, Tanaka K, Wang H, Peng D, Ren Y, Jin Q, Dent SY, Li W, Li H, Shi X. AF9 YEATS domain links histone acetylation to DOT1L-mediated H3K79 methylation. Cell. 2014;159: 558-71. doi: 10.1016/j.cell.2014.09.049.

185. Iizuka M, Stillman B. Histone acetyltransferase HBO1 interacts with the ORC1 subunit of the human initiator protein. J Biol Chem. 1999;274: 23027-34.

186. Katoh M, Katoh M. Comparative integromics on JMJD1C gene encoding histone demethylase: conserved POU5F1 binding site elucidating mechanism of JMJD1C expression in undifferentiated ES cells and diffuse-type gastric cancer. Int J Oncol. 2007;31: 219-23.

187. González-Herrera L, Valenzuela A, Marchal JA, Lorente JA, Villanueva E. Studies on RNA integrity and gene expression in human myocardial tissue, pericardial fluid and blood, and its postmortem stability. Forensic Sci Int. 2013; 232: 218-28.

188. Coyle RC, Latimer A, Jessen JR. Membrane-type 1 matrix metalloproteinase regulates cell migration during zebrafish gastrulation: evidence for an interaction with non-canonical Wnt signaling. Exp Cell Res. 2008;314: 2150-62. doi: 10.1016/j.yexcr.2008.03.010.

189. Gérard A, Patino-Lopez G, Beemiller P, Nambiar R, Ben-Aissa K, Liu Y, Totah FJ, Tyska MJ, Shaw S, Krummel MF. Detection of rare antigen-presenting cells through T cell-intrinsic meandering motility, mediated by *Myo1g*. Cell. 2014;15: 492-505. doi: 10.1016/j.cell.2014.05.044.

190. Müller T, Rumpel E, Hradetzky S, Bollig F, Wegner H, Blumenthal A, Greinacher A, Endlich K, Endlich N. Non-muscle myosin IIA is required for the development of the zebrafish glomerulus. Kidney Int. 2011;80: 1055-63. doi: 10.1038/ki.2011.256.

191. Ang Peng Hwa, Tekwani Shyam, Wang Guozhen. Shutting down the mobile phone and the downfall of Nepalese society, economy and politics. Pacific Affairs. 2012, 85: 547-561.

192. Sauer Hanno. Can't We All Disagree More Constructively? Moral Foundations, Moral Reasoning, and Political Disagreement. Neuroethics. 2015, 8: 153-169.

193. Pahwa S, Scoglio C, Scala A. Abruptness of cascade failures in power grids. Sci Rep. 2014, 4: 3694. doi: 10.1038/srep03694.

194. Mattson MP, Chan SL. Calcium orchestrates apoptosis. Nat Cell Biol. 2003, 5: 1041-3.

195. Lang F, Föller M, Lang KS, Lang PA, Ritter M, Gulbins E, Vereninov A, Huber SM. Ion channels in cell proliferation and apoptotic cell death. J Membr Biol. 2005, 205: 147-57.

1692 196. Kauffman, Stuart A. The origins of order: self-organization and selection in
1693   evolution. New York: Oxford University Press; 1993.

1694 197. Tu Y,Stolovitzky G, Klein U.Quantitative noise analysis for gene expression
1695   microarray experiments. Proc Natl Acad Sci USA. 2002, 99: 14031.

1696 198. Jackson ES, Wayland MT, Fitzgerald W, Bahn S. A microarray data analysis
1697   framework for postmortem tissues. Methods 2005, 37: 247-60.

1698 199. Barash Y, Dehan E, Krupsky M, Franklin W, Geraci M, Friedman N, Kaminski N.
1699   Comparative analysis of algorithms for signal quantitation from oligonucleotide
1700   microarrays. Bioinform. 2004, 20: 839.

1701 200. Seo J, Bakay M, Chen YW, Hilmer S, Shneiderman B, Hoffman EP. Interactively
1702   optimizing signal-to-noise ratios in expression profiling: project-specific algorithm
1703   selection and detection p-value weighting in Affymetrix microarrays. Bioinform.
1704   2004, 20: 2534.

1705 201. Harr B, Schlötterer C, Comparison of algorithms for the analysis of Affymetrix
1706   microarray data as evaluated by co-expression of genes in known operons. Nucl
1707   Acids Res. 2006, 34: e8.

1708 202. Millenaar FF, Okyere J, May ST, van Zanten M, Voesenek LA, Peeters AJ. How to
1709   decide? Different methods of calculating gene expression from short
1710   oligonucleotide array data will give different results. BMC Bioinform. 2006, 7:
1711   137.

1712 203. Amend AS, Seifert KA, Bruns TD. Quantifying microbial communities with 454
1713   pyrosequencing: does read abundance count? Mol Ecol. 2010, 19: 5555.

1714 204. Aberg F, Pukkala E, Höckerstedt K, Sankila R, Isoniemi H. Risk of malignant
1715   neoplasms after liver transplantation: a population-based study. Liver Transpl.
1716   2008, 14: 1428-36.

1717 205. Haagsma EB, Hagens VE, Schaapveld M, van den Berg AP, de Vries EG,
1718   Klompmaker IJ, Slooff MJ, Jansen PL. Increased cancer risk after liver
1719   transplantation: a population-based study. J Hepatol. 2001, 34: 84-91.
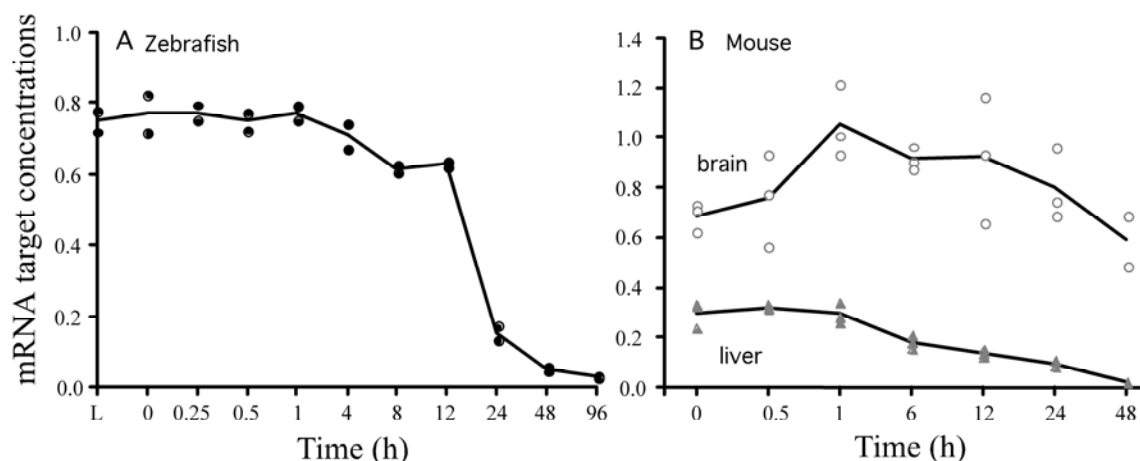
1720   FIGURES AND TABLES

1721

1722

Figure 12.Total mRNA abundance by postmortem time determined using all calibrated microarray probes. A, extracted from whole zebrafish; B, extracted from brain and liver tissues of whole mice. Each datum point represents the mRNA from two organisms in the zebrafish and a single organism in the mouse.
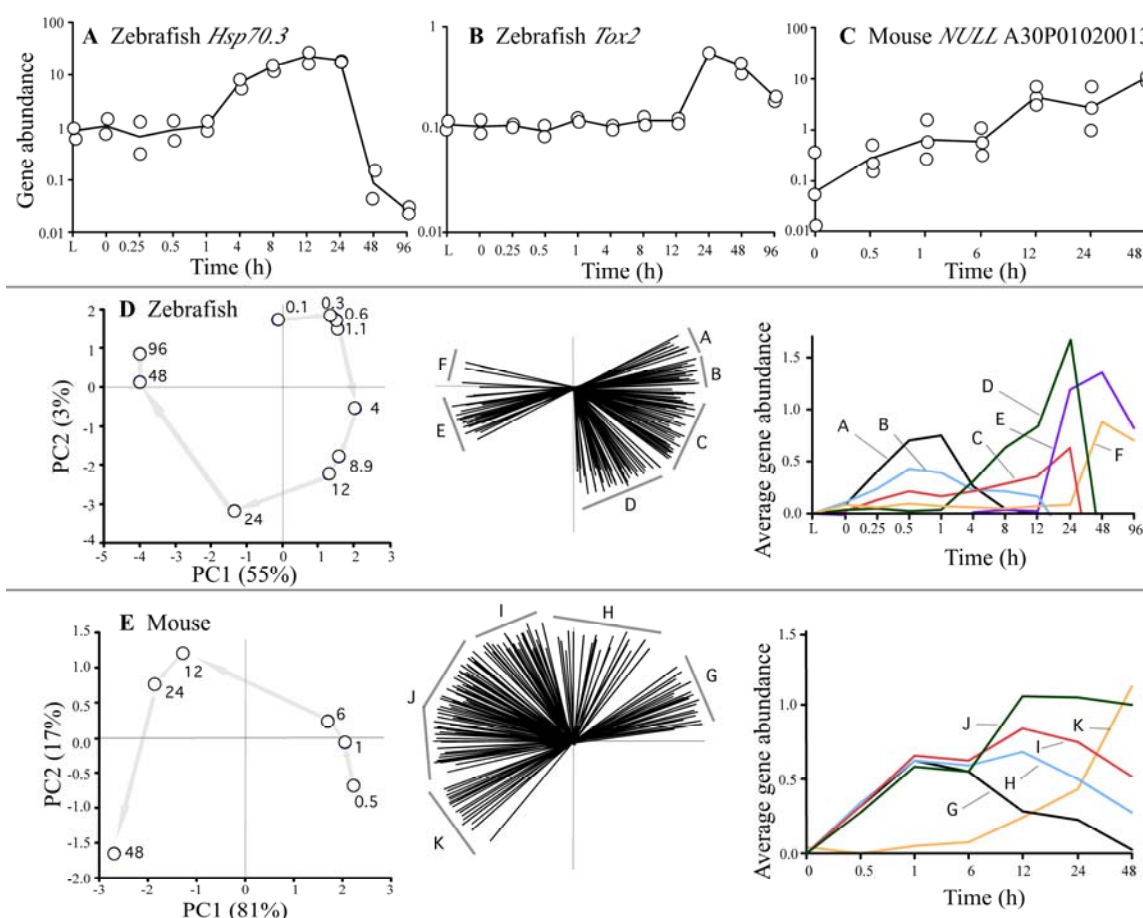
1723
1724
1725
1726

1727

1728

1729

Figure 13. Transcriptional profiles of representative genes, ordination plots based on gene abundances by postmortem time (h) with corresponding gene contributions (biplots), and averaged gene abundances by group. (A) Transcriptional profile of the *Hsp70.3* gene, (B) the *Tox2* gene, and (C) the NULL (i.e., no annotation, probe number shown) gene as a function of postmortem time. Each datum point was derived from the mRNA of two zebrafish or one mouse. (D) Ordination plots of the zebrafish and (E) mouse were based on all upregulated gene profiles by postmortem time (h). Genes in the biplots were arbitrarily assigned alphabetical groups based on their positions in the ordination. The average gene abundances for each group are shown.
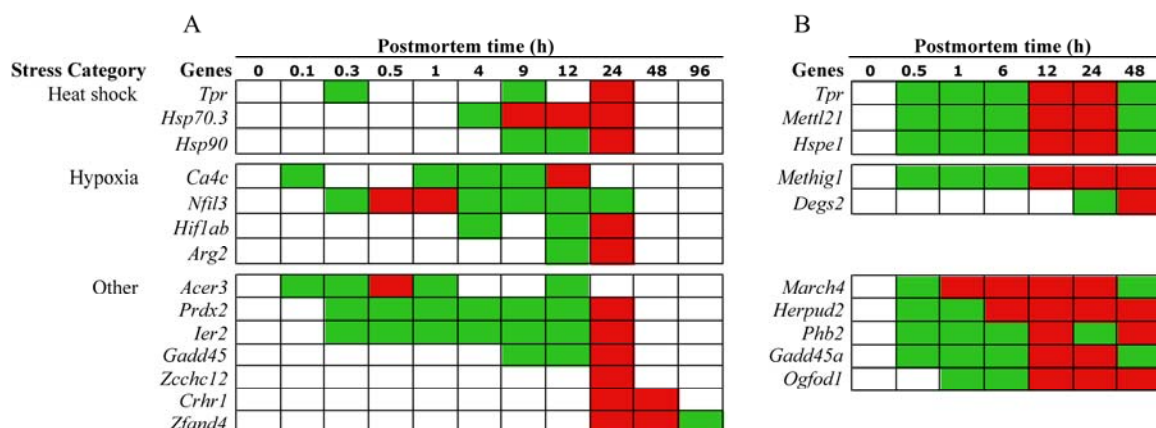
1740

1741

1742

1743

Figure 14. Upregulated stress response genes by postmortem time (h) and stress category. A. zebrafish; B, mouse. Green, intermediate value; Red, maximum value.
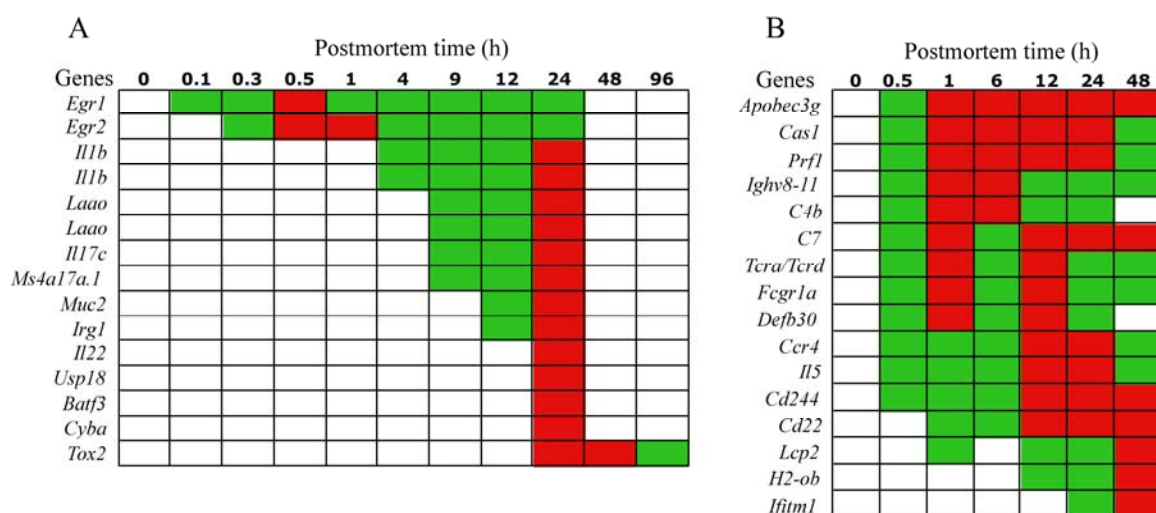
1746

1747

Figure 15. Upregulated immunity genes by postmortem time (h). A. zebrafish; B, mouse. Green, intermediate value; Red, maximum value. Some genes were represented by two different probes (e.g. *Il1b, Laao*).
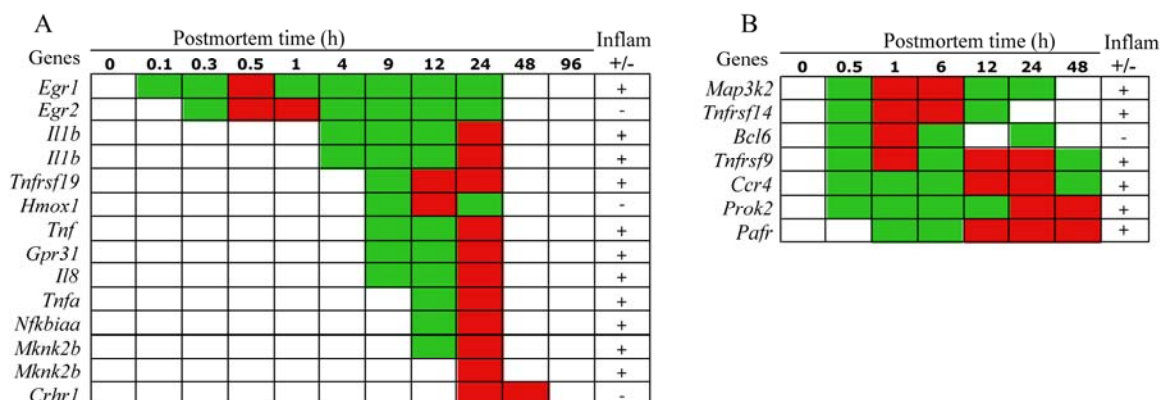
1751

1752 **Figure 16. Upregulated inflammation genes by postmortem time (h). A. zebrafish;**
1753 **B, mouse. Inflammation, Pro-, + ; Anti, - . Green, intermediate value; Red,**
1754 **maximum value. The *Il1b* and *Mknk2b* genes were represented by two different**
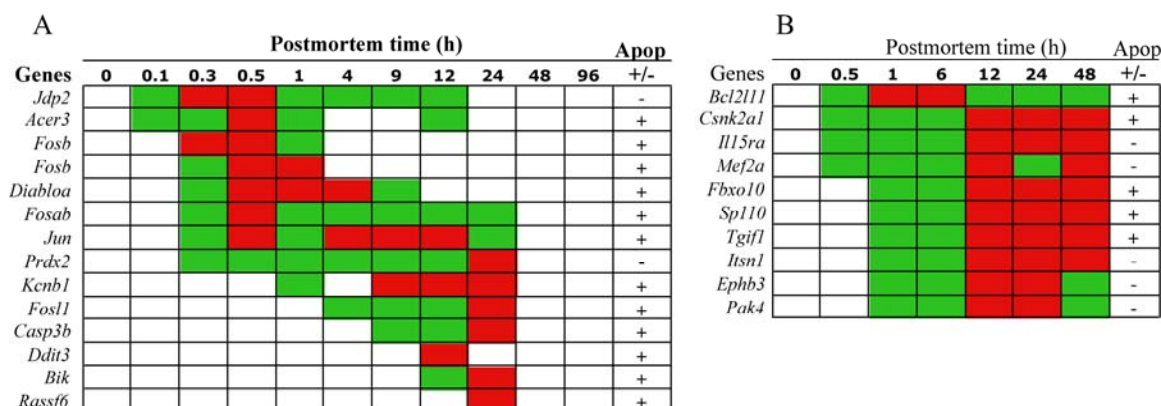1755 **probes.**

1756

1758 **Figure 17. Upregulated apoptosis genes by postmortem time (h). A. zebrafish; B,**
1759 **mouse. Apopotosis, Pro, + ; Anti, - . Green, intermediate value; Red, maximum**
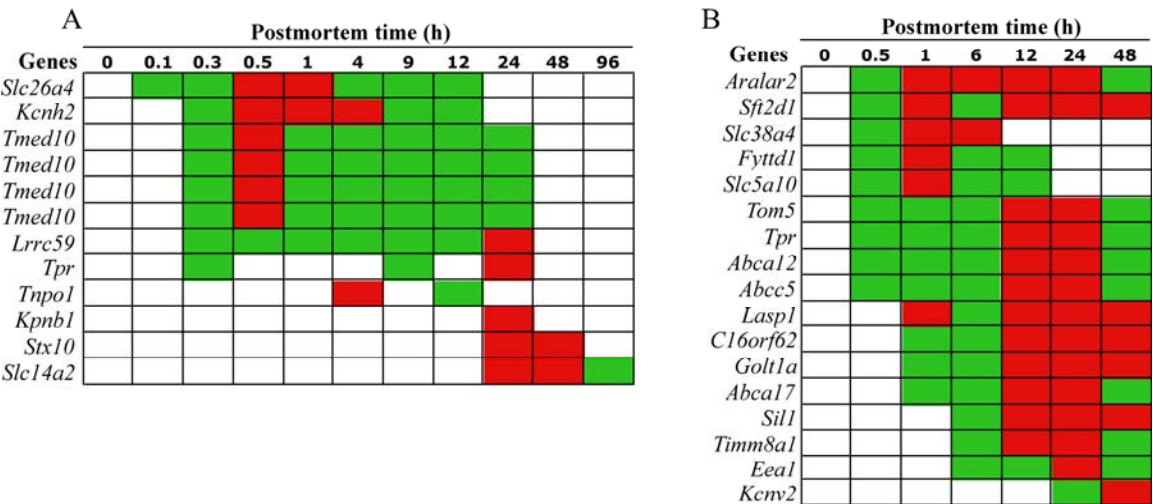1760 **value. The *Fosb* gene was represented by two different probes.**

1761

1762

Figure 18. Upregulated transport genes by postmortem time (h) and stress category. A. zebrafish; B, mouse. Green, intermediate value; Red, maximum value. The *Tmed10* gene was represented by four different probes.

1763
1764
1765
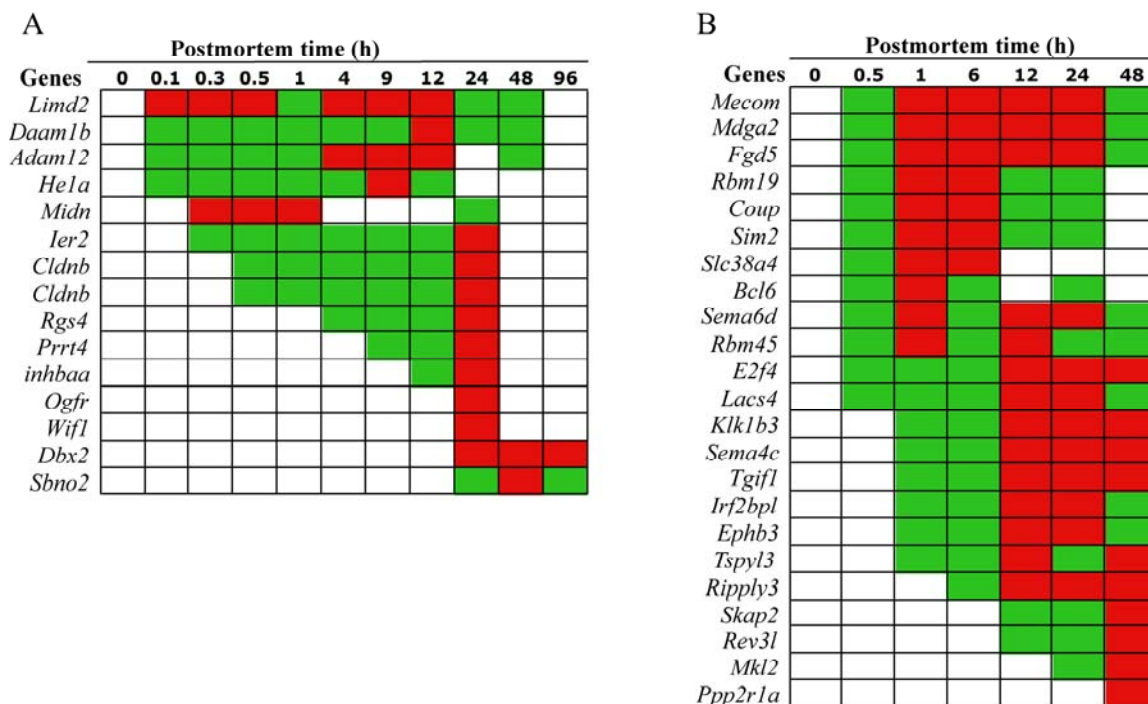1766
1767

1768
1769

1770

Figure 19. Upregulated development genes by postmortem time (h) and stress category. A. zebrafish; B, mouse. Green, intermediate value; Red, maximum value. The *Cldnb* gene was represented by two different probes.
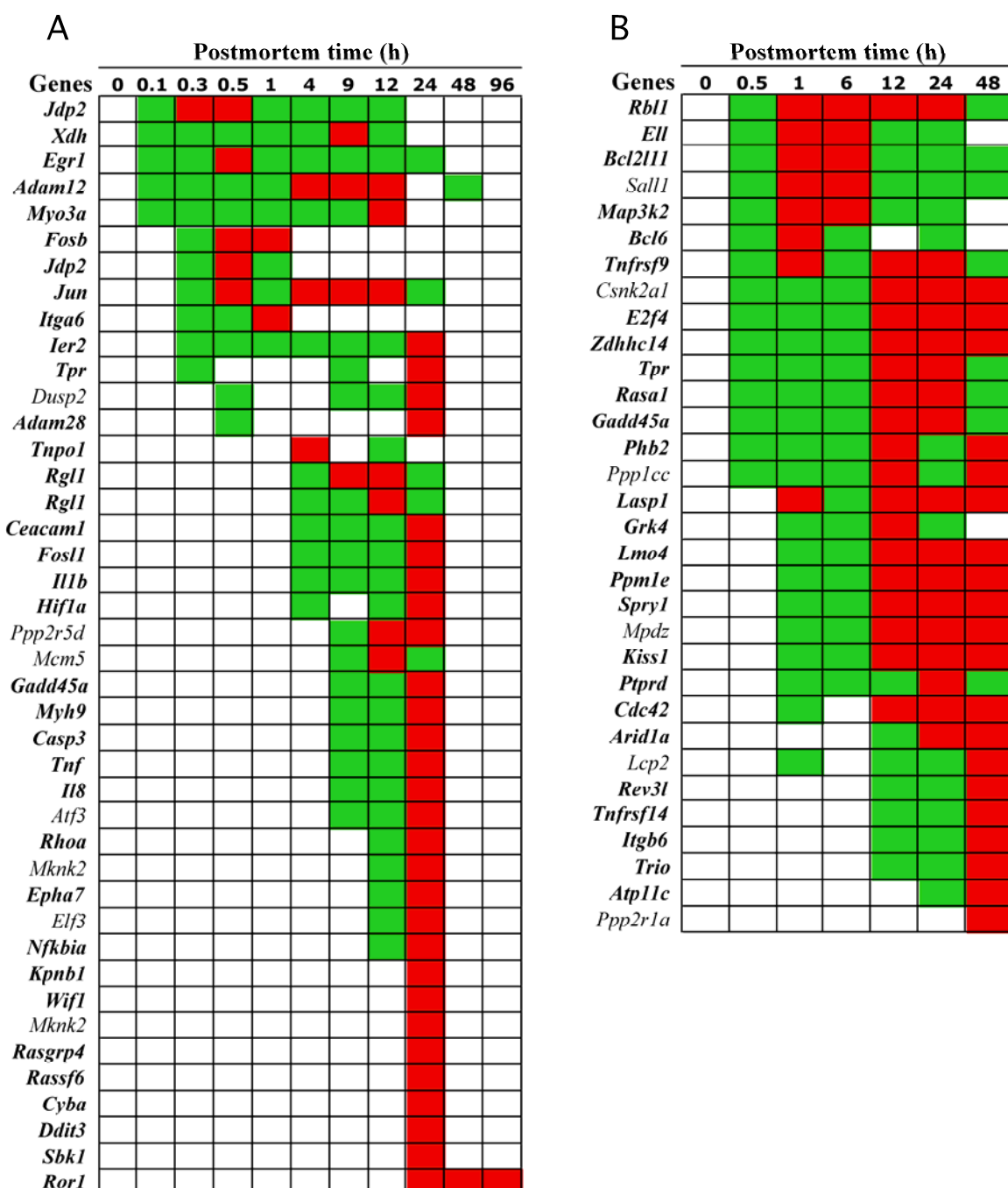
49

Figure 20. Upregulated cancer genes by postmortem time (h). A, Zebrafish; B, Mouse. Green, intermediate value; Red, maximum value. Bold gene name means it was found in more than one cancer database. The *Rgl1* gene was represented by two different probes.

A

Postmortem time (h)

Genes	0	0.1	0.3	0.5	1	4	9	12	24	48	96
Jdp2		Green	Red	Red	Green	Green	Green	Green			
Jdp2			Green	Red	Green						
Chd3			Green	Red	Green	Green	Green	Green	Green		
Grwd1					Green	Green	Green		Red		
Histh1l						Green	Green	Green	Red		
Cbx7a								Green	Red		
Hist1h46l3						Green	Green	Green	Red		

B

Postmortem time (h)

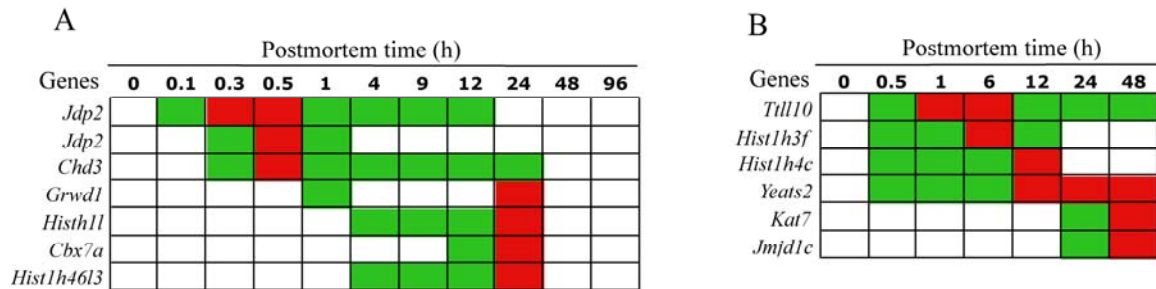| Genes	0	0.5	1	6	12	24	48
Ttll10		Green	Red	Red	Green	Green	Green
Hist1h3f	Green	Green	Red	Green			
Hist1h4c	Green	Green	Green	Red			
Yeats2	Green	Green	Green	Red	Red	Red	Red
Kat7						Green	Red
Jmjd1c						Green	Red

Figure 21. Upregulated epigenetic genes by postmortem time (h). A, Zebrafish; B, Mouse. Green, intermediate value; Red, maximum value. Bold gene name means it was found in more than one cancer database. The *Jdp2* gene was represented by two different probes.
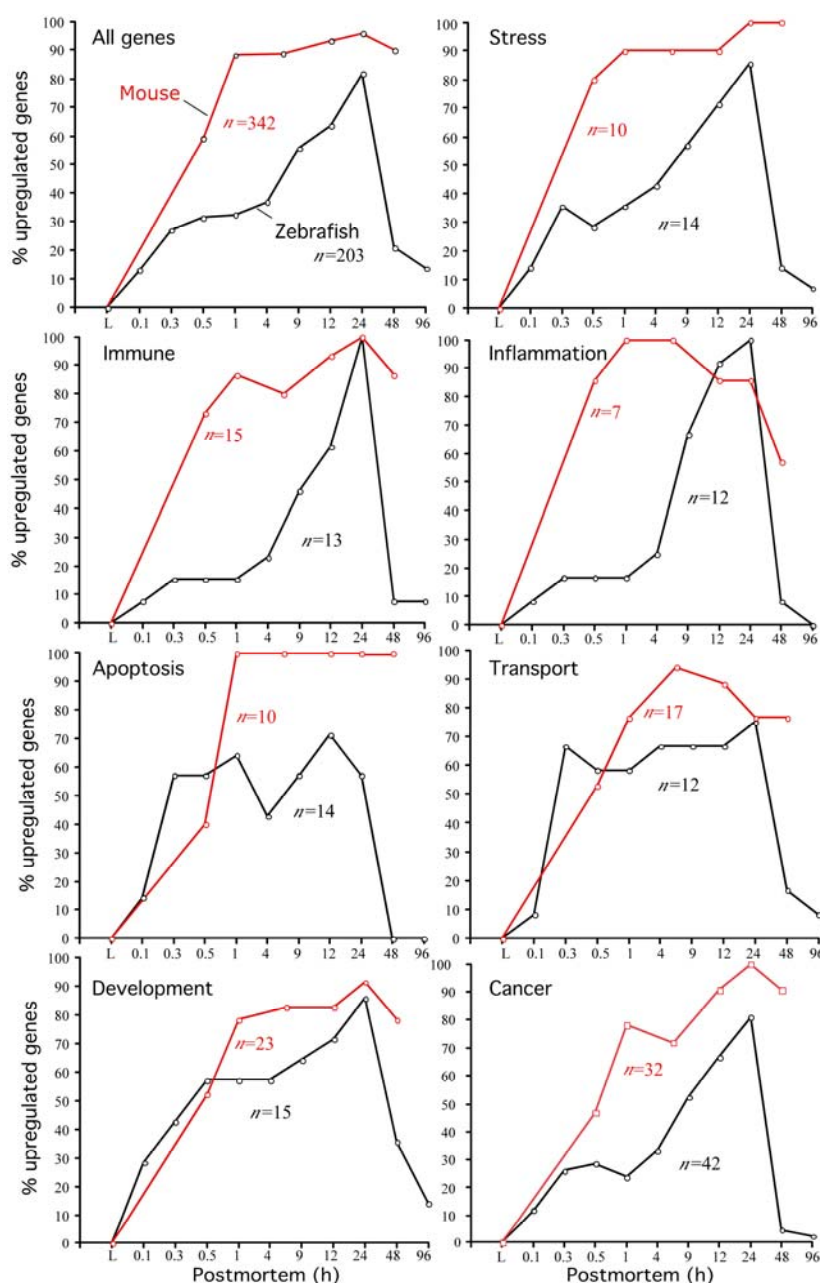
1785

1786

Figure 22. % of upregulated genes by postmortem time and category. Number of total genes by organism and category are shown. "All genes" refers to the genes that significantly contributed to the ordination plots. Mouse is red; Zebrafish is black.

Additional Files

Thanatotranscriptome: genes actively expressed after organismal death

Alex E. Pozhitkov, Rafik Neme, Tomislav Domazet-Lošo, Brian G. Leroux, Shivani Soni, Diethard Tautz and Peter A. Noble[*].

*Correspondence to: panoble@washington.edu

This PDF file includes:

Supplementary Text

Figs S1, S2 and S3

Table S1

Other Additional Files for this manuscript includes the following:

Data files S1 to S8 as zipped archives:

File S1. MiceProbesParameters.txt

File S2. FishProbesParameters.txt

File S3. Mouse_liver_Log10_AllProfiles.txt

File S4. Mouse_brain_Log10_AllProfiles.txt

File S5. Fish_Log10_AllProfiles.txt

File S6. MiceProbesSeq.txt

File S7. FishProbesSeq.txt

File S8. Gene_annotation_lit_refs_v3.xls

SUPPLEMENTARY TEXT

Fig S1. Bioanalyzer results showing total mRNA from the zebrafish.

Fig S2. Bioanalyzer results showing total mRNA from the mouse.

Fig S3. Transcriptional profiles in the zebrafish (*Acer3* gene) and mouse (*Cdc42* and *Rbm45* genes) by postmortem time.

Table S1. Total mRNA extracted (ng/µl tissue extract) from zebrafish by time and replicate sample.

Table S2. Total mRNA extracted (ng/µl tissue extract) from mouse organ/tissue by time and replicate sample.

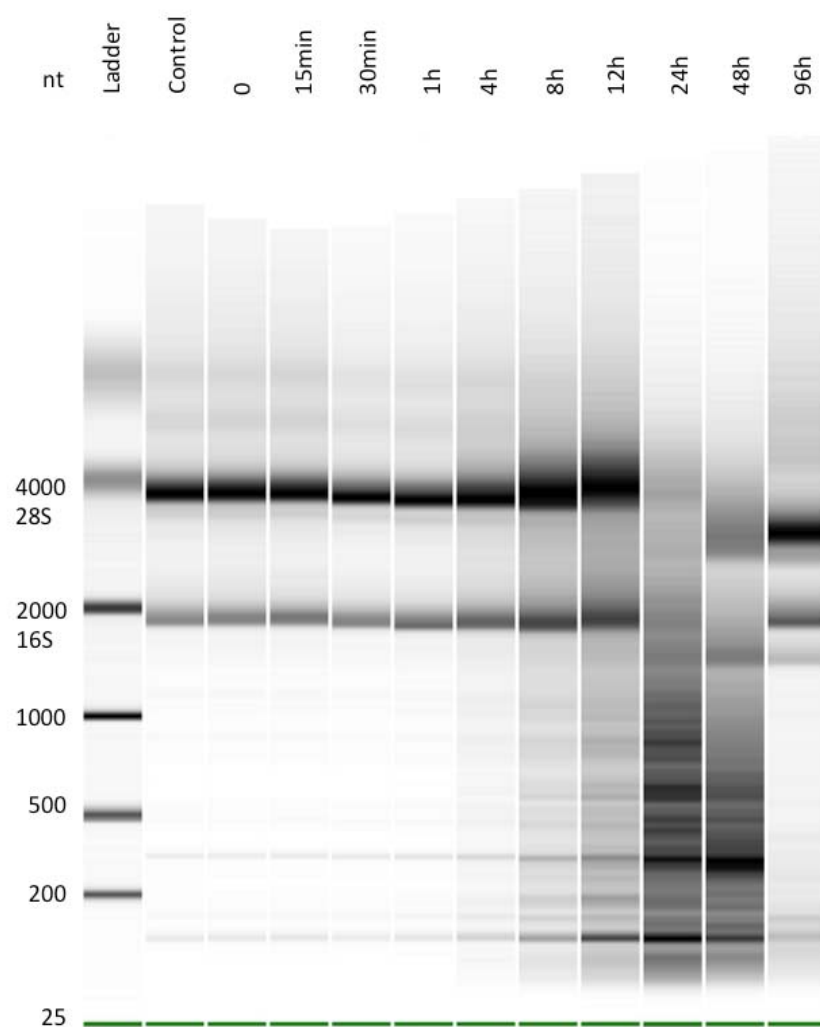Table S3. % of global regulator genes and response genes.

Fig S1. Bioanalyzer results showing total mRNA from the zebrafish. Only one replicate per sampling time is shown. The dominant bands represent the 28S and 18S rRNAs.
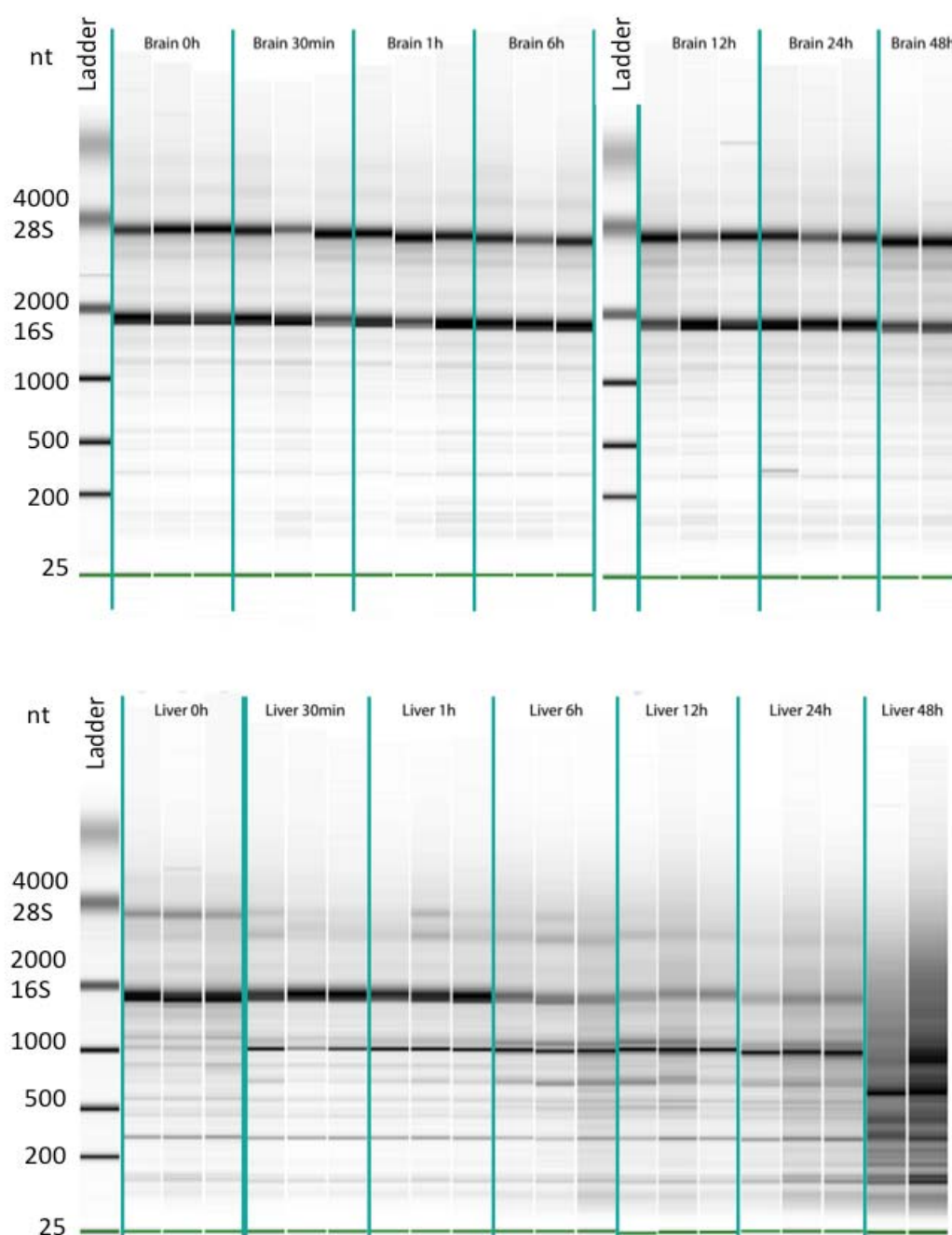
Fig S2. Bioanalyzer results showing total mRNA from the mouse. All replicates per sampling time are shown. The dominant bands represent the 28S and 18S rRNAs.
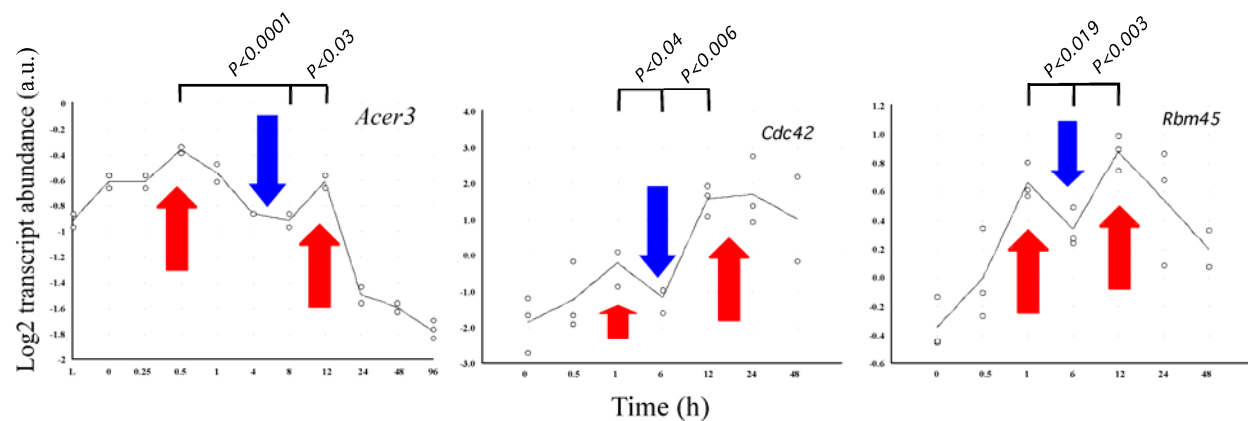
Fig S3. Transcriptional profiles in the zebrafish (*Acer3* gene) and mouse (*Cdc42* and *Rbm45* genes) by postmortem time. Red arrows, up-regulation; blue arrows, down-regulation. One-way T-tests show significant differences between means. Results suggest that the differences in up- and down regulation by postmortem time are due to changes in regulation rather than changes in "residual transcription levels".

Table S1. Total mRNA extracted (ng/µl tissue extract) from zebrafish by time and replicate sample.

Time (h)	Repl#1	Repl#2
Live	1606	1648
0	1632	1481
0.25	1768	1573
0.5	1457	1481
1	1864	1514
4	1251	1651
8	1605	1499
12	1365	1422
24	1087	539
48	339	428
96	183	183

a, no replicate taken

Table S2. Total mRNA extracted (ng/µl tissue extract) from mouse organ/tissue by time and replicate sample.

Organ	Time (h)	Repl#1	Repl#2	Repl#3
Liver	0	432	387	443
Liver	0.5	533	651	569
Liver	1	421	426	601
Liver	6	541	624	528
Liver	12	839	450	845
Liver	24	1021	510	1066
Liver	48	1453	1197	-[a]
Brain	0	169	226	210
Brain	0.5	174	166	410
Brain	1	194	485	264
Brain	6	401	269	256
Brain	12	379	258	203
Brain	24	249	324	400
Brain	48	397	310	-

a, no replicate taken

Table S3. % of global regulator genes and response genes. Approx. 33% of all upregulated genes are involved in global regulation.

Global gene regulators and other response genes	Zebrafish	Mouse	Combined
Transcription factors and transcriptional regulatory genes	17	12	14
Cell signaling genes	24	16	19
Other response genes	59	73	67